A Simulation Scheme for Strategic Distribution of Damping Coefficients

by

Sung-June Kim

Bachelor of Science in Civil Engineering
Hong-Ik University (1998)

Submitted to the Department of Civil and Enviornmental Engineering
in partial fulfillment of the requirements for the degree of

Master of Science in Civil and Environmental Engineering

at the

MASSACHUSETTS INSTITUTE OF TECHNOLOGY

May 2000

Author .....
Department of Civil and Enviornmental Engineering
May 19, 2000

Certified by .....
Jerome J. Connor
Professor of Civil and Enviornmental Engineering
Thesis Supervisor

Accepted by .....
Daniele Veneziano
Chairman, Departmental Committee on Graduate Studies

A Simulation Scheme for Strategic Distribution of Damping Coefficients

by

Sung-June Kim

Submitted to the Department of Civil and Enviornmental Engineering
on May 19, 2000, in partial fulfillment of the
requirements for the degree of
Master of Science in Civil and Environmental Engineering

Abstract

Structural design has entered a new phase during the past decade due to the implementation of structural protective devices in full scale structures. Passive, active, and adaptive control theories have been widely focused on throughout the search for efficient design. However, deciding the location for structural protective devices has somewhat been neglected or overlooked in many studies. This is partially due to the fact that there is no rational or clear cut procedure to determine the location of such devices. Thus, two strategic methods for the strategic distribution of passive energy dissipation devices through out a system are explored.

Optimality is defined on a performance based criteria: the interstory strains, which are known to be the main cause of structural deterioration. Cost efficiency, which is an important aspect, is transformed into a design constraint problem. In this attempt, a simulation design scheme based on fundamental control theory is explored: introducing various strategic indices. This method will then be compared with a more general approach, the Maximum Transfer Function (MTF) method. The latter utilizes the amplitude of the transfer function which is a general dynamic property of the system. In order to enhance the computational efficiency of the two design schemes, two different dynamic analysis methods are studied and applied: the state-space approach and the transfer function approach.

The methods are applied to 7 case studies. For each case study, results show similar trends for the different methods. In general, the simulation design is efficient in terms of computational intensity. It is also more flexible in terms of applying various constraints that must be anticipated in practical designs. However, the optimal design is governed by the strategic index that is used. As for the MTF method, the results coincide with the optimal designs obtained from the previous method. However, it lacks robustness.

Thesis Supervisor: Jerome J. Connor
Title: Professor of Civil and Enviornmental Engineering

Acknowledgments

First, I would like to express my gratitude to my advisor, Professor Jerome Connor, for his guidance, feedback and continued encouragement. His foresight and broad perspective expanded my academic horizon and helped me stumble upon the subject of my thesis.

Second, I would also like to take this opportunity to thank Professor Chongyul Yoon, my undergrad advisor, for propelling my interest in civil engineering.

Third, I would like to thank my friends and office mates who have endured me for the past two years: Daniel Dreyer, who could not stand me anymore and eventually returned to his home country, Germany; Joon-sang Park, who has given me advice and assistance since the first day at M.I.T; Karen Veroy, whose big feet has always awakened our tired labmates down in the *rat hole*; Satoshi Suzuki, who was so different from what I would have expected from a typical japanese. My gratitude also extends to Heung-soo Kim, Un-nam Park, and Andy Kim and his wife, who helped me maintain my sanity. I would also like to acknowledge my fellow countrymen in our department to whom I could whine in Korean: Moonseo Park, Seong-chul Kang, Yunsung Kim, Jungwook Hong and Saeyoon Kim. I would also like to thank my best friends in Korea, you know who you are! I know you did not do much in my work here but you were always there and you will always be there. So thank you guys, I love you.

Last, but not least, I would like to thank my parents for their affection and their huge support, and my brother for being a great role model. I know I was not the ideal kid for you, mom and dad, but you know I love you most of all.

Contents

List of Figures

List of Tables

Chapter 1

Passive Energy Dissipation Devices

1.1 Introduction

The design of structures, such as buildings, dams, and bridges, have evolved significantly since its inception. Throughout each evolutionary stages, the dominant concern of structural design was whether the particular structure would be capable of supporting its own gravity load *(dead load)* due to the heavy construction materials. This concern was one of the main reasons for the design of massive monumental structures that have been built, such as the pyramids of Egypt, and the early high-rise buildings. *Dead loads* are always present, and thus, must be considered throughout the lifetime of the structure. The variation of the load is slow compared to the characteristic times of the structure allowing engineers to idealize the problem statically. Such approaches have shown quite appropriate, leading to numerous design codes. In addition, the structure's heavy design has enabled the structure to dissipate external input energy, reducing the vibration of the structure. However, as resources have become increasingly limited and constraints on construction materials and labor costs have become issues, efficient design has now become a requirement.

Emphasis on efficiency has challenged engineers to design more sophisticated and delicate structures. Eventually this design movement opened a new generation of structures that were highly flexible and slender. However, these innovated designed structures became vulnerable to vibrations that are non-existent in heavy design structures of the past. In addition, development of new high strength construction materials has further compounded this problem by reducing the capacity of dissipation of the structure in allowing more finesse skeletons. Hence, protection against environmental loads, such as winds, earthquakes, and

various vibrations due to trains or underground facilities, has become important. These loads are not independent from time, nor unidirectional, which exacerbates the problem. Inertia forces must be considered which result in dynamic amplification in the response. Thus, compared with dead loads, since the temporal and spatial scales of these phenomena are much smaller, they are much more difficult to predict. However, considering the actual dynamic characteristics of the applied external loads would lead to a more sophisticated, efficient, and improved design. As engineers have followed down this path of design prospective, new and innovative concepts of structural protection have been advanced and developed.

	Structural Protective Systems
Passive Devices	Base-isolation, Tuned mass dampers (TMD), Tuned liquid dampers (TLD), Tuned liquid column dampers (TLCD) Passive energy dissipation device
Active Devices	Active tuned mass damper, Active variable stiffness device
Adaptive Devices	Neural network, Fuzzy logic, Expert systems implemented in the control algorithm, Smart materials

Table 1.1: Structural Protective Systems

Modern structural protective systems can be largely divided into three categories, as illustrated in Table. (1.1).

Isolation technique has gained favorable status in aseismic design throughout many parts of the world. This particular technique places isolation systems at the bottom or foundation of the structure. It forms a cushion between the earthquake-induced input energy and the structure. This helps to reduce the amount of energy the structure has to dissipate, which as a result, reduces the energy dissipation demand of the structure. Eventually, increasing the longevity of the structure's life span. However, long sways in the structure's response is inevitable. The objective of the structure's design will help solve the dilemma between

safety of the structure and human/equipment comfort. Tuned mass dampers (TMD) is a technique that uses the effect of a out-of-phase mass to govern the response of the structure. The energy dissipation is due to the damper's inertia force acting on the structure. This technique has been widely used to reduce wind/ground vibrations of tall slender buildings.

Active and Adaptive control systems are a new area of protective systems for the large structures in civil engineering compared to those of mechanical and aerospace structures. Passive energy devices have fixed properties, which enables the system to react to a unpredicted load instantaneously. Considering these disadvantages, and efforts to improve the performance, by dynamically modifying the system properties, have led to active and adaptive control systems. These systems require external energy supplies to activate the control system to reduce or control the motion of the structure. However, active control systems require only nominal amounts of energy to adjust their mechanical properties and unlike fully adaptive control systems, they cannot apply or add energy to the structure. There has been extensive research in this field and the technology is now at the stage of implementation for full-scale structures.

Active mass dampers are similar to the previously mentioned TMD. They only differ in that TMD's masses are driven by actuators that are controlled by the main control system. An active variable stiffness (AVS) device is a non-resonant control system. By continuously varying the stiffness of the building to avoid the resonant state, it reduces the input energy induced by the external excitation. The advantage of this non-resonant system is that it requires a small amount of input energy to activate the system, which is a problem for most active/adaptive control systems.

An adaptive system may be described as active control systems with varying control and properties. Ultimately improving the dynamic modification of the control system to unpredicted loads. The main control system checks and adjusts its control algorithm instantaneously to the external excitation. This control scheme requires sophisticated control algorithms, such as Neural Networks, Fuzzy Logic, and Expert Systems.

The technologies that have been briefly presented are adequate to effectively reduce motion and will take on important roles in the next generation of civil structural design. Among these technologies, it is not controversial that adaptive control systems will be most widely used in the future. The following are prerequisites to enable adaptive control systems to be commercially viable:

- Development of civil structure type: adaptive materials, sensors, and actuators
- Improvement of control schemes: efficient and robust control algorithms and fast computational computers
- Safety Requirements: Emergency Power Supply must be a available, Durability/Reliability & Repair ability must be conformed

1.2 Passive Energy Dissipation Devices

Passive energy dissipation devices, which have been in research and development for over 25 years, are the crux of the study. These devices vary in size and capacity ranging from 30 cm to 3m, they are incorporated between frames or the diagonal of braces of the structure to dissipate or consume input energy for the primary structure. They have been proved to be effective for wind loads as well as seismic loads and do not require external energy supplies for the system to work. Here are some passive energy dissipation devices that are widely used.

1.2.1 Metallic Dampers

The first 'passive energy dissipation device' mentioned here is the metallic damper, which is a very effective mechanism that uses the inelastic deformation (*hysteric behavior*) of metallic substances. Devices that utilize flexure, shear, or extensional deformation in the plastic range have been developed. Stable behavior, long-term reliability, and good endurance to environmental and thermal conditions are the advantages of these sort of devices. Kelly et al (1972) and Skinner et al (1975) first initialized this concept of utilizing separate metallic hysteric dissipation devices.

Conventional steel design for aseismic design is based on pot-yield ductility of the structural members to provide the required dissipation capacity for the input energy. In addition devices which function as integral parts of seismic isolation systems have been developed. Tyler (1985) developed a device, from round steel bars, for cross-braced structures as shown in Fig. (1-1). Energy is dissipated by inelastic deformation of the rectangular steel frame in the diagonal direction of the tension brace. In order to include these devices into the overall design process effectively, we must characterize their expected nonlinear force-displacement

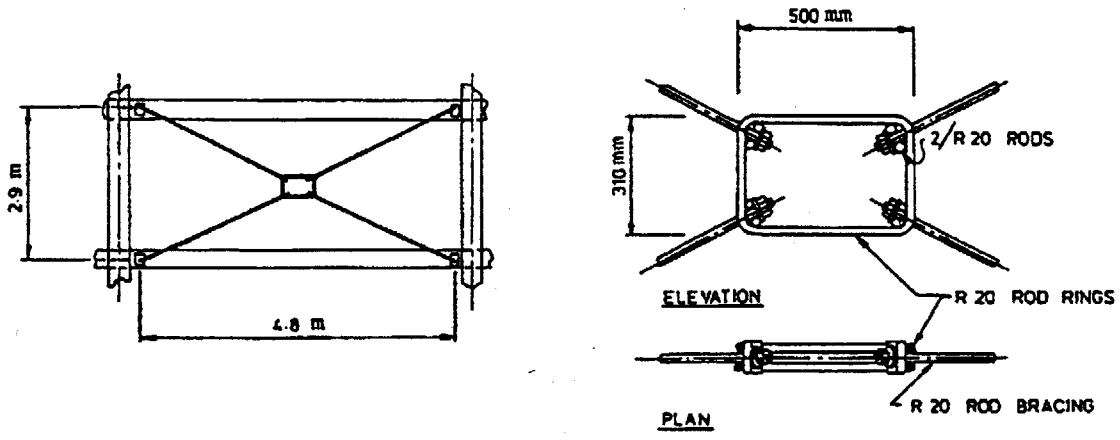

Figure 1-1: Yielding steel bracing system (after Tyler, 1985)

behavior under arbitrary cyclic loads. Once the force-displacement model is established for the given device the design engineer must incorporate that information in the analysis of the overall structural design. In the development of the force-displacement relationship, there are couple of different approaches that may be pursued. One is to approach it empirically, by studying the experimental data obtained from numerous testing of the devices. However, requiring experimental data for each damper configuration and size, as well as having no direct link between the model parameter and damper geometry is a demerit. An alternative approach is using the principles of mechanics that will characterize the overall force-displacement relationship from a constitutive model of the metal along with a geometric description of the device. Hence, giving a more comprehensive understanding of its performance within a structural system. Excessive experiments have been explored while new designs have been proposed, such as X-shaped braces and triangular plate dampers. the most common material has been mild steel although alternative materials have also been in the research interest. Lead and shape-memory alloys are just some to be mentioned.

1.2.2 Friction Dampers

The friction dampers differ from the previous presented metallic dampers such that, while the latter uses the mechanism of *internal friction* the former utilizes the mechanism of *solid friction* to gain the required energy dissipation capacity. Friction between 2 solid bodies

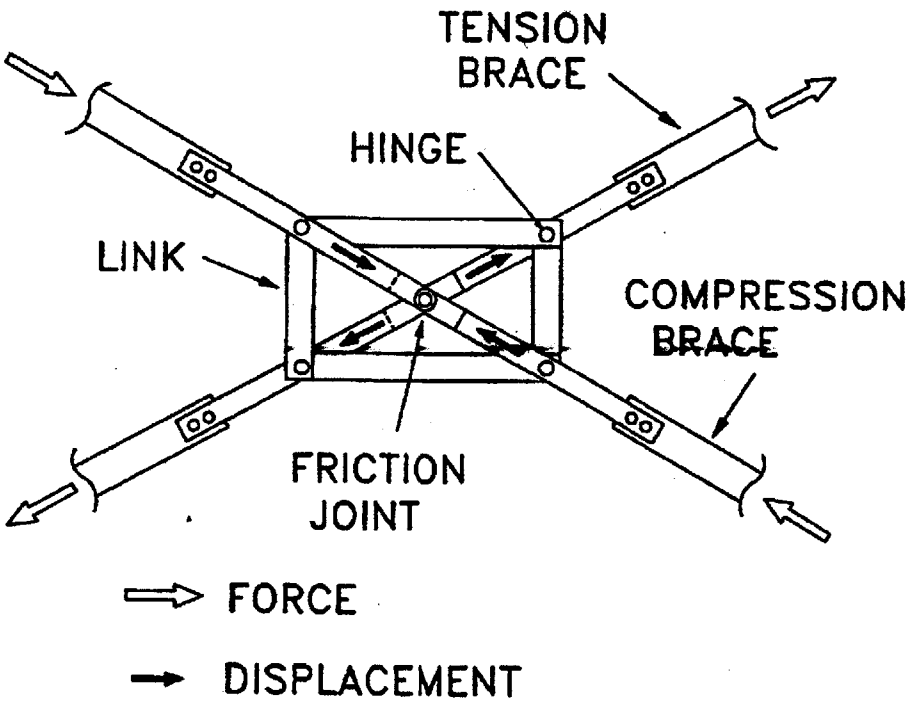

Figure 1-2: Pall friction damper (after Pall and Marsh, 1982)

sliding relatively to one another has been widely used in engineering fields. For one well-known example is the brake of an automobile. Thus, this analogy from the automobile brakes to a passive energy dissipation device for aseismic structural design was initialized by Pall et al (1980). The objective is to slow down the motion of building by braking rather than breaking' (Pall and Marsh, 1982).

Fig. (1-2) is a device that is located at the intersection of cross bracings in frames. The tension brace induces slippage at the friction joint when loaded. This lead by the four links, induces the compression brace to slip. Thus, energy is dissipated in both braces in both tension and compression.

Numerous mechanisms exist in the form of friction that can be effective for energy dissipation devices. However, the importance to have a consistent, predictable and working frictional mechanism through out the life of the device is crucial. For example, dry, sliding, solid friction devices generally require the contacting surfaces to remain dry during the period it is in use, while environmental causes may effect the designed mechanism and hence, the device may not function to the required capacity it was initially designed.

Thus, the importance to consider environmental effects is a prior. Physiochemical processes that may occur in the interfacial region often triggered by atmospheric moisture or contaminants, are most of the concern. By altering the physical and chemical characters of the surface, this phenomenon may produce a significant change in the frictional response along the surface. However, for the type of systems that are employed in most frictional dampers, it is unlikely to effect the response of the system.

Generally, these devices have good performance, and their behavior is less affected by the load frequency, number of load by cycles, or variations in temperature.

1.2.3 Viscoelastic Dampers

Viscoelastic materials have been implemented in structures for use of vibration control since the 1950's when it was first used in the aeronautics field for controlling vibration-induced fatigue in airframes (Ross et al., 1959). It has been continuously favored widely in aircraft and aerospace structures for vibration control ever since. However, it's first application to civil engineering structures was in 1969 when 10,000 viscoelastic dampers were installed in each of the twin towers of the World Trade Center in New York to help reduce vibration due to wind loads (Mahmoodi, 1969 Mahmoodi et al., 1987; Caldwell, 1986). Contrast to wind load applications, seismic applications of viscoelastic dampers have a more recent origin. The necessity for a larger damping capacity compared with wind applications and the requirement for a more effective use of the material due to the wider frequency range of the energy input must have been the main reason. After extensive analytical and experimental studies in the seismic application first building installed with viscoelastic dampers in the U.S. was erected in 1993, nearly 15 years after the World Trade Center. The viscoelastic materials used in energy dissipation devices in structural applications are mostly copolymers or glassy substances which dissipate energy while deforming in shear. A typical VE shear damper consists of viscoelastic layers bonded to steel plates. The energy dissipation takes place when the structural vibration induces relative motion between the center plate and the outer steel flanges, due to shear deformation.

The stress-strain relationship can be expressed as,

$$\gamma(t) = \gamma_0 e^{i\omega t}, \quad \tau(t) = \tau_0 e^{i(\omega t+\delta)} \tag{1.1}$$

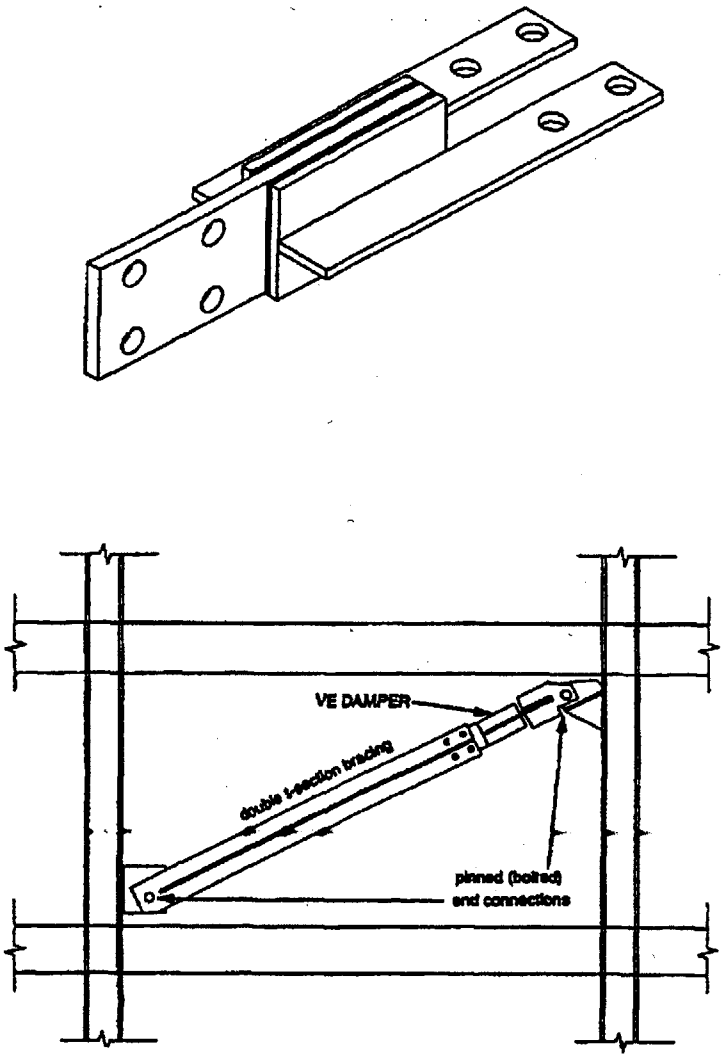

Figure 1-3: Viscoelastic damper and installation (after Aiken et al., 1990)

under a sinusoidal load with a frequency ω, where, $\gamma(t), \tau(t)$ can be both expressed in terms of the peak stress γ_0 and strain τ_0. δ is the lag (phase) angle between the shear stress and shear strain.

$$\tau(t) = G^*(\omega)\gamma(t) \tag{1.2}$$

where G^* is the complex modulus of the viscoelastic material,

$$G^*(\omega) = G'(\omega) + iG''(\omega) = G'(\omega)(1 + i\eta) \tag{1.3}$$

$G'(\omega)$ and η, determine the dynamic behavior of the linear viscoelastic material in shear under time harmonic excitation. These moduli are functions of excitation frequency ω, ambient temperature and shear strain. In order to evaluate the property of the viscoelastic damper is the variation of internal temperature within the material during operation since energy is dissipated in the form of heat, giving rise to temperature rise in the viscoelastic material. The damper properties are also dependent on the number of loading cycles and the range of deformation, especially under large strain due to temperature increase within the damper material. One of the most serious problems with viscoelastic devices is an unacceptable increase in force at low temperatures coupled with an accompanying overloading of the bonding agent used to 'glue' the viscoelastic material to its steel attachments. At high temperatures, unacceptable softening or reduction of output occurs. This thermal variance from high to low temperature can be a very important defect.

1.2.4 Viscous Fluid Dampers

The Viscous fluid Dampers differs itself from the previous energy dissipation devices by not utilizing inelastic deformation. However, Viscous Fluid Dampers have proven to be very effective in their applications to vibration mitigation in structures. The concept for a fluid damper for general vibration mitigation is well known, for example, shock absorbers in cars. Recently, the development towards viscous fluid dampers for structural applications has been intense.

Fluid Viscous damping reduces stress and deflection because the force from the damping is completely out of phase with stresses due to flexing of the columns. This is only true with fluid viscous damping, where damping force varies with stroking velocity. Other types of damping such as yielding elements, friction devices, plastic hinges, and visco-elastic elastomers do not vary their output with velocity; hence they can, and usually do, increase column stress while reducing deflection. Viscoelastic devices have an output that is somewhere between that of a damper and a spring. Under high level seismic inputs, the spring response dominates, producing a response that increases column stresses at any given deflection. This does not happen with Fluid Viscous Dampers. Consider a building shaking laterally back and forth during a seismic event. Column stress is at a maximum when the building has flexed a maximum amount from its normal position. This is also the point at which the flexed column reverses direction to move back in the opposite direction. If we

add a Fluid Viscous Damper to the building, damping force will drop to zero at this point of maximum deflection. This is because the damper stroking velocity goes to zero as the column reverses direction. As the building flexes back in the opposite direction, maximum damper force occurs at maximum velocity, which occurs when the column flexes through its normal, upright position. This is also the point where column stresses are at a minimum. It is this out of phase response that is the most desirable feature of fluid viscous damping.

There are 3 basic types of viscous fluid dampers. The first device mentioned here directly emulates the dash-pot. Dissipation occurs via conversion of mechanical energy to heat as a piston deforms a thick, highly viscous substance. Very often ribs and other geometric details are included in the design of the piston to enhance performance. The energy dissipates in all degrees of freedom due to the axisymmetric configuration.

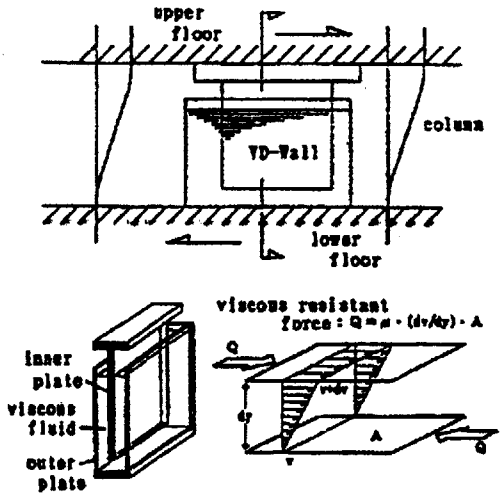

Figure 1-4: Viscous Damping Wall (after Miyazaki and Mitsusaka, 1992)

An alternative and perhaps more effective design concept is the viscous damping wall (VDW), which was developed by Sumitomo Construction Company, Japan. The basic mechanic of this device is simple. The piston is simply a steel plate constrained to move in it's plane within a narrow rectangular steel filled with a viscous fluid. The piston is attached to the upper floor, while the container is fixed to the lower floor. Relative inter-story drifts provides shear to the fluid which produces energy dissipation. The viscous damping force is induced by the relative velocity between the two floors. However, in order to maximize the energy dissipation density of these devices, large viscosity materials must be incorporated.

This evidently utilizes materials that dependent on both frequency and temperature.

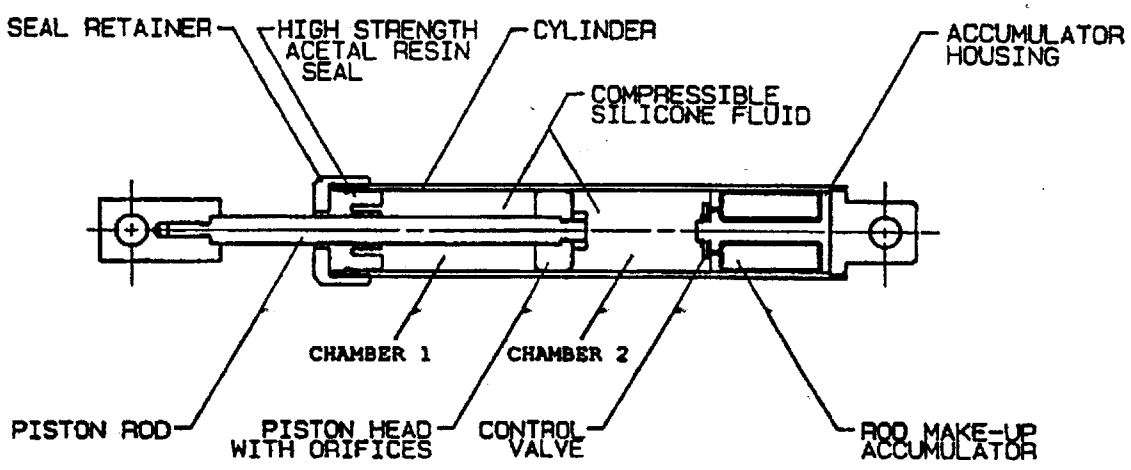

Figure 1-5: Construction of fluid viscous damper (after Constantinou and Symans, 1992)

Another type of fluid damper is a device, which operate on the flow of fluids through orifices. The force in the damper is generated by a pressure differential across the piston head. Now, the piston forces the fluid to pass through a small orifice. This allows extremely high amount of energy dissipation density to be obtained. To compensate for temperature changes a fluidic control orifice designed with a passive bimetallic thermostat is installed in the head. In addition, to compensate for the change in volume due to rod positioning an accumulator is provided.

1.3 Thesis Overview

The objective of this thesis is to first compare and evaluate a simulation design approach and a search technique (MTF), which minimizes the maximum absolute amplitude of the transfer function, to strategically position passive energy dissipation devices. We formulate the problem as to find the optimal distribution of the damping coefficients, when given a specific mass and stiffness distribution. *Optimality* is defined as obtaining the better response: performance based. The simulation design scheme requires external excitations, while the MTF method is a general solution technique that does not rely on external excitations.

In Chapter 2, the 2 design schemes, simulation design and search technique, are intro-

duced. Each of the designs' strategic concept, design procedure, and implementations of design constraints are revised. Chapter 3 deals with the dynamic analysis tool, which differs in each method. A modified state-space approach is used in the simulation design, while, the structure is modified as a chain joint structure to obtain the transfer functions in the search technique. The evaluation and comparison of the two proposed methods is covered in Chapter 4. While, the summary and comments of the study is given in Chapter 5.

Chapter 2

Strategic Placement of Energy Dissipation Devices

2.1 Introduction

An important issue in the new design concept, which incorporates energy dissipation devices in the primary structure, is the strategic positioning of devices. However, research on optimal energy dissipation devices have been very limited.

Constantinou and Tadjbakhsh derived the optimum damping coefficient for a damper placed on the first story of a shear building subjected to horizontal random earthquake motions. Gurgoze and Muller presented a numerical method for finding the optimal placement and the optimal damping coefficient for a single viscous damper in a prescribed linear multi-degree-of freedom system. Zhang and Soong proposed a seismic design method to find the optimal positioning of viscous dampers for a building with specified story stiffness. While their method is based on an intuitive method, it has been appreciated as pioneering. We will discuss this intuitive method more thoroughly in the following section. Hahn and Sathiabageeswaran performed several parametric studies on the effects of damper distribution on the earthquake response of shear buildings and showed that, for a structure with a uniformly distributed stiffness, dampers should be added to the lower half floors of the building. De Silva suggested a gradient algorithm for the optimal design problem, focused on vibration control of flexible systems. Inaudi and Kelly proposed a procedure for finding the optimal isolation damping for minimum acceleration response of base-isolated structures

subjected to stationary random excitation. Tsuji and Nakamura proposed an algorithm to find both the optimal story stiffness distribution and the optimal damper distribution for a shear building model subjected to a set of spectrum-compatible earthquakes. Connor and Blink proposed a design scheme that suggests the optimal stiffness distribution and the optimal damper distribution through out a building, while incorporating the bending effects to the typical shear beam model. This methodology attacks the problem with basic dynamic properties. Suggesting that the engineer should protect the fundamental mode that is estimated to be excited, and allow some cushion by protecting additional modes. The methodology also emphasizes the damping effect on stiffness distribution, such as the more damping provided to the building the less stiffness required.

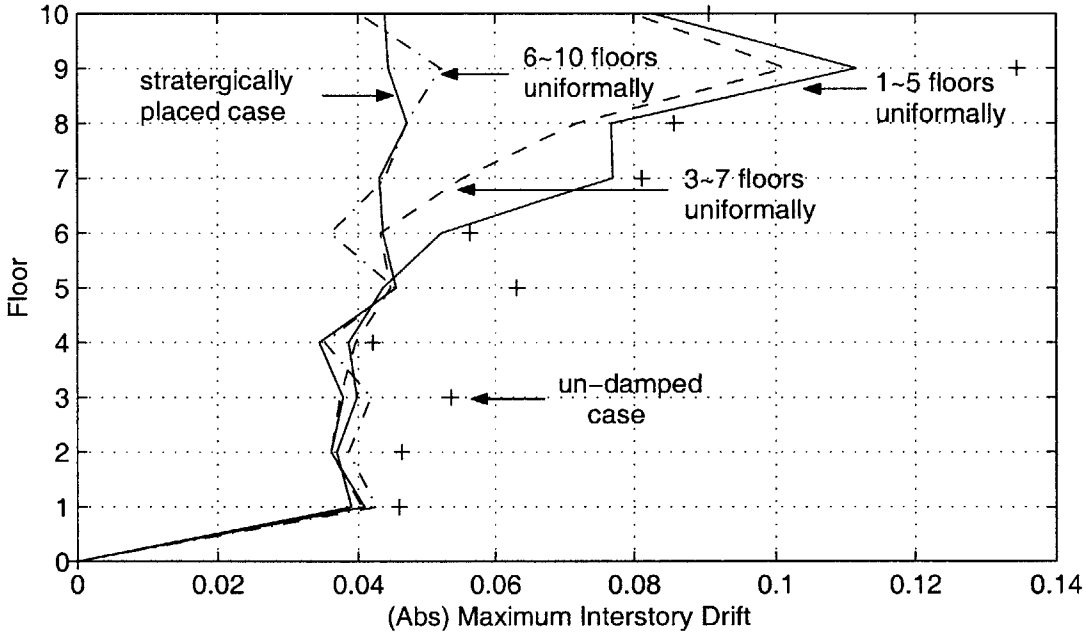

Figure 2-1: Comparison of Absolute values of Maximum Inter-story Drift of 5 cases

The vibration of a structure can be divided largely into 3 regions. Governing parameters of a given structure transists from stiffness, damping, and last the mass of the primary structure. Here, we define the given design problem such that the earthquake occurs after the building is fully erected and established. This indicates that the structure's stiffness (**K**) and mass (**M**) is fixed and we are now to identify the preferable locations of the passive energy dissipation devices which are to be installed. We are to modify the region where the damping governs the structure. Placement of dampers are determined by the characteristics

of the structure and by the load's property. This Means that the solution of placements of dampers strongly depend on the given design problem, such as anticipated excitation's characteristic. However, this does indicate that there exist more preferable places than others, in placing dampers through out the structure.

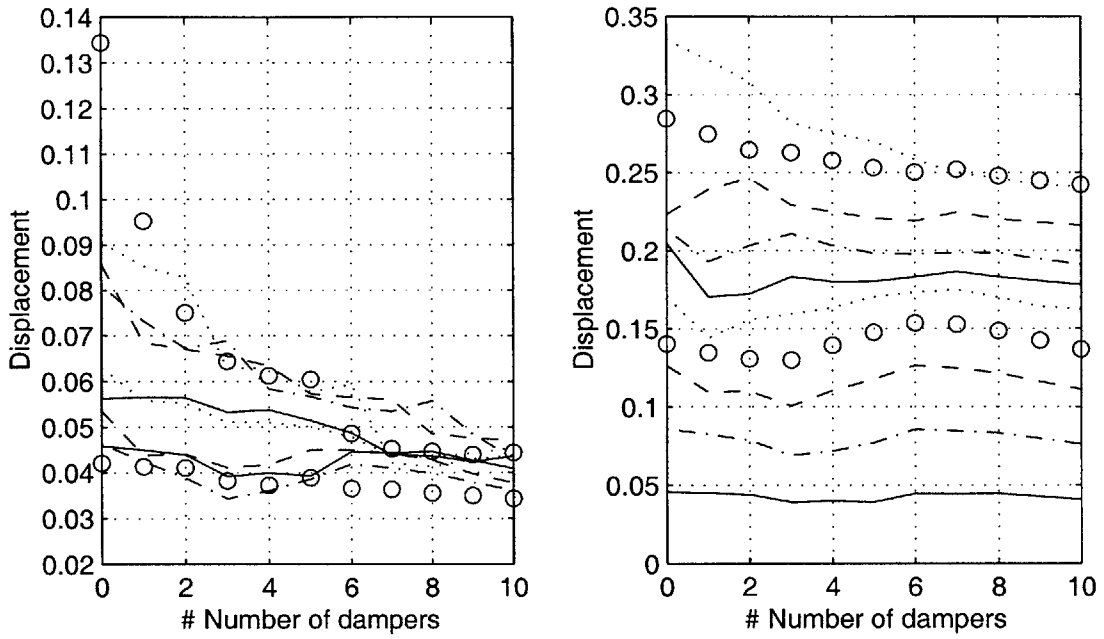

Figure 2-2: Reducement of Maximum Inter-story drift by strategically placed viscous-elastic dampers: (a) Inter-story drift (b) Relative displacement

In Fig. (2-1) 10 dampers are placed in a 10 story building type model. The absolute maximum values of the inter-story drifts are compared for 5 cases. The undamped case and the cases where 10 dampers were equally distributed throughout floors $1 \sim 5$, $3 \sim 7$ and $6 \sim 10$. And of course the strategically placed case where damper placement was chosen in sequence, after detecting the maximum inter-story drift each time a damper was placed. In this case 3 dampers were placed on the 7^{th} and 9^{th} floor, 2 dampers on the 8^{th} and 10^{th}. Even though the dampers were concentrated highly in the upper floors Fig. (2-1) shows that there does exist a preferable distribution in allocating the dampers through out the structure under a given load. Fig. (2-2) shows that attacking the floor with maximum inter-story drift does effect the structure in a efficient way. However, we may point out that even though the maximum inter-story drift is reducing remarkably,

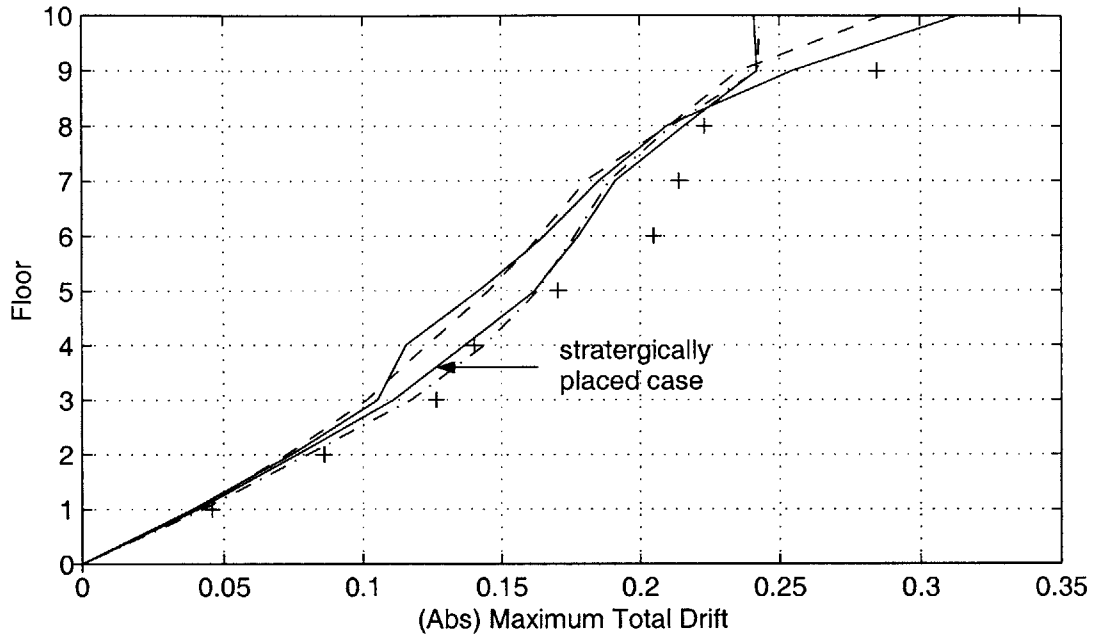

Figure 2-3: Comparison of Absolute maximum story drifts

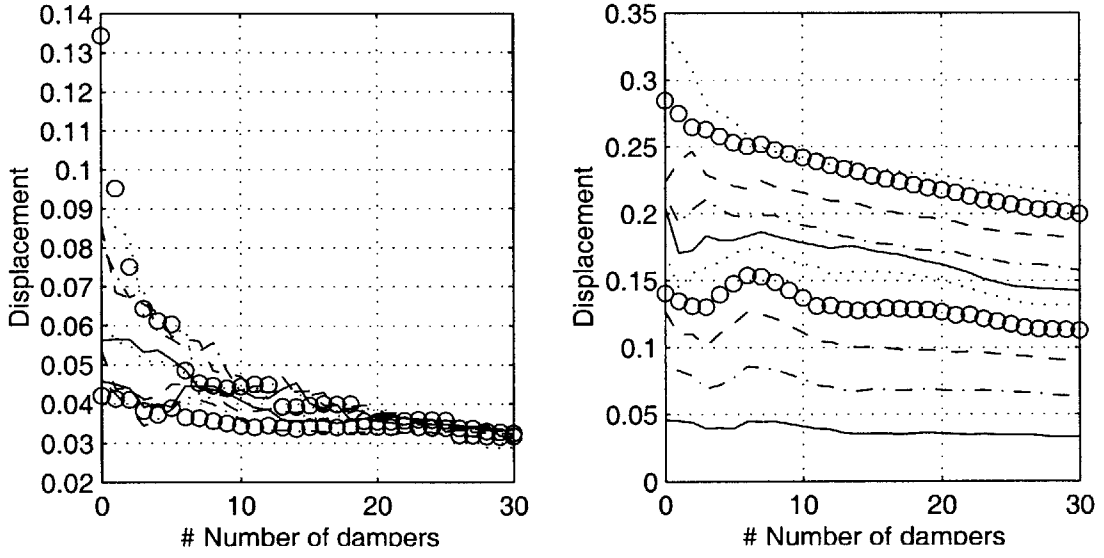

Figure 2-4: Reducement of effectiveness of adding dampers: (a) Interstory drift (b) Relative displacement

the maximum total displacement of a floor seems to have not been affected with the placement of dampers. This can be shown in Fig. (2-3) as well. As the strategic case lies somewhat in between the other examined cases. Fig. (2-4) shows that there exists a upper limit for how many dampers are effective for a given structure under a specified load. As the number of installed dampers exceed 18, the effectiveness of an additional damper has diminished. This complicates the problem for design, when we start considering cost functions. However, this study will not deal with the aforementioned problem.

In this study we examine 2 different approaches for the optimal location of dampers problem. The first is positioning devices due to strategic indices, which indicate preferable places focused on the anticipated external excitation. While, the other approach was a more general step to enhance the devices effectiveness, by dealing with general dynamic properties of the structure.

2.2 Simulation Design

While, previous studies have approached the optimum placements of dampers problem quite effectively there still exists some limitations. First, the uncontrolled modes of the structure have been repeatedly used to find the optimal locations. These locations have been found at once without consideration of the effects of high damping ratio: when the damping ratio is considerably high, damping alters the mode shapes of the structure and thus changes the optimal locations of the devices. Second, to be able to position a device anywhere the strategic index indicates, the engineer must not be constrained with conventional damping, i.e., proportional damping. In addition to proportional damping previous studies have used only a few lower modes to optimize the locations of the devices. Although the lower modes contributions are enormously high, higher modes may be important for typical structures under specific excitations. Important enough when dealing with the problem of optimal placement of dampers. This emphasizes the need for an accurate dynamic analysis approach. In addition to these limitations the design must provide the optimal damping ratio for each mode. This could be easy for proportional damping or for a single degree of freedom problem, however, for a multi-degree of freedom with non-proportional damping this itself can be considered as a problem.

The objective of this study is to overcome these limitations and requirements to ul-

timately provide an effective and economic distribution of energy dissipation devices in a given structure. In order to fulfill this goal a *simulation design* procedure is proposed and compared with an alternative approach which uses the general dynamic property, i.e., the amplitude of the transfer function, by reducing the maximum transfer function in the excited mode due to the service load.

2.2.1 Main Concept

The main concept of the *Simulation Design Procedure* is based on the optimal placements of actuators in control theory. First, proposed by Cheng et al(1980), then modified by Zhang and Soong et al(1993) [11] for passive energy dissipation devices. Intuitively suggesting that the next energy dissipation device's optimum placement should be decided based on the previous selections. With the presumption that the previous placement was the 'optimum'. The optimal location of the device is determined with the help of the strategic index, which usually represents a measurement worth to be controlled.

The overall idea behind the sequential procedure is that a passive energy dissipation device is optimally located if it is placed at where the strategic index of the uncontrolled or modified structure indicates. The strategic location of the first device is determined from the uncontrolled response of the structure. After adding the energy dissipation device, the procedure is repeated by taking the modified structure as the primary structure and reanalyzing the response to determine the optimal location for the next device. This procedure is repeated until all energy devices are installed in the structure. However, the extent of the presumption's validity is yet to be determined. After placing an additional damper, say the n^{th} damper; it is questionable whether we can still suggest the previous n-1 dampers still be in the most optimum locations for the n^{th} case.

Here we formulate the design problem as a deterministic problem, such that we have our design loads as grouped earthquakes that can represent a geological location. Using an ensemble of earthquakes that represent a region is an admissible approach. We use the simulation design procedure, comparing certain strategic indices such as maximum inter-story drifts (MID), maximum inter-story velocity (MIV), maximum reduction ratio (MRR).

2.2.2 Strategic Indices

Depending on the design criteria, there can be various strategic indices. For an example, the root mean square (RMS) represents a physical meaning, the response of the stochastic process, and by dividing it with the story height will give the inter-story strain of the structure. While interpreting the RMS value as a strategic index and by controlling this index would be meaningful.

Maximum Inter-story Drift (MID)

This procedure is a straightforward approach by placing energy dissipation devices where the largest inter-story strain occurs during the simulation of the excitation. Assuming that the floor with the largest inter-story strain in the structure during the excitation is the most critical place, thus indicating that an energy dissipation device should be effective when installed in that floor. Here, we express the strategic indices with σ,

$$\sigma_d = max(v_i) \tag{2.1}$$

where, v denotes inter-story drift, and i indicates that this index serves for the i_{th} damper.

For undamped structures the peak displacement is proportional to the absolute peak acceleration, which is also a crucial design criteria for motion based design structures. However, here we are directly using the inter-story drifts and not the relative displacement of the structure in the dynamic analysis such that we are not directly controlling the absolute peak acceleration simultaneously. None the less, it will be easy to transform the formula presented here for the latter proposed design criteria.

Maximum Inter-story Velocity (MIV)

Numerous studies have shown that placing dampers where the largest displacement occurs is efficient. However, it can be also as efficient when devices are placed at the floor with the maximum inter-story velocity, due to the characteristic of the structure. This is a procedure suggested based on the definition that a linear viscous damper's force is proportional to the inter-story velocity.

$$\sigma_v = max(\dot{v}_i) \tag{2.2}$$

where, the $\dot{v}$ indicates the inter-story velocity. This may be similar to the friction damper's objective to slow down the motion of the vibrating structure.

An interesting prospect of these two proposed strategic indices may be that one seems to govern the state of the structure than the other. Such that, when implementing a weight factor for the two values, we can capture a more preferable strategic placement for the dissipation devices.

Maximum Reduction Ratio (MRR)

Placing a passive energy dissipation device between a floor will have an effect on the shear flow throughout the structure and eventually effect the response of the structure. This was shown in the previous chapter which discussed over the impulse response. Thus, now our strategic index is

$$\sigma_{mrr} = max(mrr) = max\left[\frac{max(\text{v w/o additional damper})}{max(\text{v w/ additional damper})}\right] \tag{2.3}$$

Not like the previous proposed strategic indices, the MRR finds the strategic placement of the device by trying all the available floors and then comparing the obtained results. The modified structure which gives the minimum response is chosen. With this newly modified structure the process is repeated till all the devices are placed.

This approach does seem to find very efficient positions of the energy dissipation device on behalf of the sequential procedure. However, no analytical explanation on how to find the index directly has been found. This would be where fast computational dynamic analysis schemes would highly contribute in the design process. The computational intensity approximately is n times higher than the previously proposed strategic indices, where n is the number of Degrees-of-Freedom's in the design problem, or the number of possibilities of a placement of a damper.

2.2.3 Simulation Design Process

The design process is:

Step 1. Initial Design Properties

- Given initial structural properties

- Given representation of excitation
- Define the sum of damping coefficients $\mathfrak{C}$
- Define design criteria
- Define structural/architectural constraints
- Define strategic index: MID, MIV, MRR, MDV

Step 2. Simulation and Data Analysis

- Simulate under defined excitations
- Obtain (ensemble) responses: inter-story strains, inter-story velocities, etc,...
- Obtain strategic index

Step 3. Installation of damping coefficient Δc: Compare response with design criteria:

- If N.G: install Δc, and return to Step 2
- If O.K: end design process
- If $\sum c > \mathfrak{C}$: end design process

Step 4. Ultimate Design: Compare response with design criteria:

- If O.K: design is successful
- If N.G: return to Step 1 and redesign

It is straight forward and easy to implement various design constraints in the design process. This is an advantage which previous studies have failed.

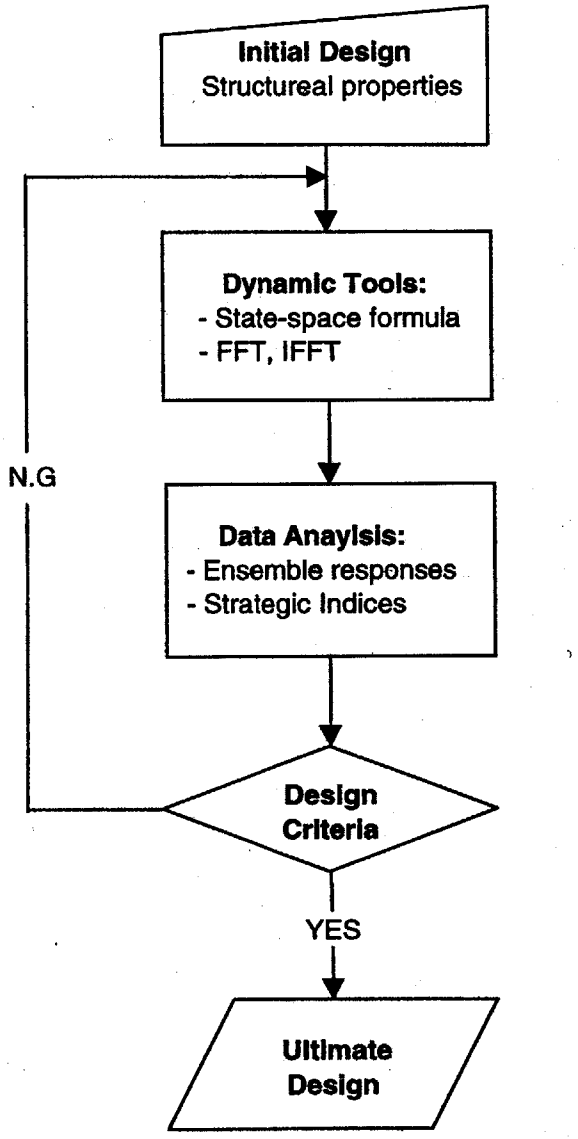

Figure 2-5: Flowchart: Simulation Design

2.2.4 Dynamic Analysis Tool

The general goal of this study is to be allowed to put an active or passive device freely, wherever and whenever it is needed. Thus, to be able to adapt with the new design concept efficiently, we must not constrain ourselves with problems like non-proportional damping. This is one of the reasons the *State-Space* approach is used as the dynamic analysis tool in this study.

State-space analysis is very efficient with dealing with non-proportional damping. It also has other advantages, such as having inter-story and relative velocity and also the same for displacements as outputs. Turning the general 2^{nd} order equation into a 1^{st} order equation, which most engineers are more comfortable with, also gives a reason that make this approach attractive. And last, not like modal superposition, which neglects higher modes, it solves for the exact solution. However, there's always the other side of the coin and with the state-space formulation, it is the non-symmetric matrix form of the state space coefficients. Thus, the need for solving the non-symmetric eigenvalue problem is a requirement. This directly affects the computational intensity of the problem, as for civil engineers who must deal with massive amount of DOF's, this would become a problem if not dealt with more concern. However, when dealing with strategic placements of passive energy dissipation devices, such as Visco-Elastic Dampers (VED) it would be preferred to deal with the inter-story drift as our output. This alters the general *equation of motion* into a non-symmetric eigenvalue problem, thus we are already dealing with an non-symmetric problem.

The design starts with the initial design properties (undamped) of the structure, as indicated in Fig. (2.2.3). Then the dynamic analysis of the structure is executed for each design excitation. Thus, if n earthquakes were taken for the design, n responses are obtained. It is then followed with the preceding procedures. It will repeat this cycle until the design criteria is satisfied. Each time with an additional damper placed at the proposed position.

2.2.5 Data Analysis

To ensemble responses from groups of earthquakes that represent a geographical location is an admissible design approach. By taking several past earthquakes from the region and seeking the response of the structure will provide an approximate estimation on how the

structure will behave on a upcoming earthquake excitation. However, the lack of sufficient earthquake data is a problem for more sophisticated design. Other options are to consider the earthquake's ground acceleration as a stationary stochastic process with a zero-mean and a power spectral density function (PSDF). Where the PSDF is expressed with ω_g, ε_g, and S, which are parameters that depend on the intensities and characteristics of earthquakes in a particular geological location. However, this is just another estimate of an earthquake of a geological location. In this study the earthquakes are scaled by its peak acceleration.

Another step in data analysis is 'how to ensemble the simulated responses?' This is where the decision making of the design procedure steps in. In this study due to the fact that only 4 earthquakes are used for the representation of the geological region, taking the mean values of the response shows to be more efficient than taking the maximum values. However, if more earthquake datum are available, more sophisticated probability analysis of the obtained responses might be preferable.

After receiving the responses from the simulation process, the mean value of the maximum responses become the strategic indices. By comparing the strategic indices we obtain the strategic index for the next energy dissipation device. The next procedure is the implementation of the design criteria.

2.2.6 Design Criteria

This is the final step in the simulation design procedure for a cycle. It is here whether the structure is determined, corresponding to the it design criteria, safe or not. Should the design criteria not been satisfied by this point the iteration process will continue. The iteration process continues till all the devices are considered to have been placed.

In current earthquake engineering procedures, structures are provided with a minimum strength based on a fraction, (I/R), times the theoretical lateral strength demand that would be experienced were the structure to remain elastic. The occupancy importance factor, I, is introduced into the base shear as a modifier on the response modification coefficient, R. However, the R factors have been set based on judgment and in part, based on observation of structural performance in recent earthquakes, to provide the so-called life safety performance level for design level earthquake ground motions. This life safety level of performance has been defined only qualitatively in terms of poorly stated considerations of limiting damage to structural elements, maintaining egress for occupants, and preventing

significant falling hazards. Both SEAOC's Vision 2000 (SEAOC, 1995) and the NEHRP Guidelines (ATC, 1996) have attempted to provide more quantitative definitions of building performance levels. To hold the structure in elastic regions and simplify the problem, we impose a performance based criteria, which holds the inter-story strain within 1/200.

It is also at this stage where constraints of the design can been easily employed. The iteration design process is controlled by either 3 options. This differs from previous studies where the amount of dampers where verified previously before the distribution of devices were determined.

- constraints on initial design
- structural constraints on the building
- architectural constraints

The first is by the constraints on the initial guess of amounts of devices required. Such that if the design is only capable of n dampers the iteration process will stop after n iterations even if the design criteria has not been satisfied. In this case the designing engineer will acknowledge that the design has not satisfied the design criteria and will modify the design: change the stiffness distribution or mass properties or even increase damping.

Structural constraints on the building must also be considered in the design process. Such that on each floor there is a limit on the amount of total dampers that can be installed. The number of bays throughout a story, the actual size of the structure will also be considered.

Architectural constraints are somewhat related to the previous structural constraint. However, differs from the point of view that this is employed due to artistic or other such issues that are not related to feasibility due to the actual structure design. This will be more to the functionality of the structure.

These are just several constraints that in the design process engineers might confront. It has been difficult in other studies to employ these sort of constraints efficiently. Thus, most studies tend to have neglected these obstacles. This eventually shows that this simulation design scheme also provides the optimal number of dampers for the given structure, simultaneously. Which is why this procedure is so efficient.

Cost Consideration

Cost factor, as well as performance, is an essential element and constraint in design. However, to consider this additional factor in the design scheme is not a trivial procedure.

While evaluating the distribution of the damping coefficients, the cost factors have been transformed into a constraint problem in order to be considered in the problem. Costs of damping devices accelerates as the required capacity of a device increases, thus, by introducing specific constraints in the algorithm we may encapture the aspects of cost efficiency. This will allow the design process to block out heavy concentration of damping in a given floor.

This would just be a slight variation from the previously mentioned constraints. Hence, the actual implementation of all the constraints will eventually mold into one constraint on each floor of the system.

2.3 Minimization of the Transfer function

2.3.1 Main Concept

Transfer functions are general dynamic characteristics of the structure. For a single-degree of freedom (SDOF), reducing the amplitude of the transfer function directly reduces the response of the system due to external excitation. For multi-degree of freedom (MDOF) systems implementing this general dynamic characteristic is not that simple. Controlling the amplitude of the transfer function provides a general solution to random vibrations. It should be noted that the squares of the amplitudes of the transfer functions have a physical meaning. They can be transformed into the root mean squares (RMS), which are statistical quantities after being multiplied with the power spectral density function (PSDF) of an earthquake and integrated in the whole frequency domain. Thus, This could provide a procedure for a stochastic design approach, which would differ from the previous deterministic load.

The problem of optimum placement of dampers is sort of a inverse problem. Various studies have been done on inverse eigenmode problems of undamped systems. Takewaki [13] (1997) proposed a systematic procedure for finding the optimal damper placement by finding the damping coefficients of added dampers which minimize the sum of *amplitudes* of the transfer functions of the inter-story drifts. These transfer functions were obtained from

the undamped structure. The results are general and are not influenced by characteristics of the external excitation.

2.3.2 Search Technique

The problem is to define the optimal distribution of a given number of energy dissipation devices. Where *optimality* means the minimization of the maximum amplitudes of the transfer functions of the structure. To solve this problem with a more general approach we use the general dynamics characteristic, reduction of the transfer function. However, to obtain an efficient and an effective systematic method to obtain the transfer functions, we utilize the impulse response. The methodology is dealt in the latter part of Chapter 3.

A *search technique* is used to obtain the minimum of the transfer functions for a given structure. We first conceptually consist a function, or a n dimensional space, which is consisted with the maximum amplitude of the transfer function of the system. The damping coefficients are the variables of the function. Our main objective is to find the distribution of the damping coefficients which gives the minimum point of this function. Different from the previous solution technique the search technique must start with implementing an initial guess. This is due to the non-linearity of the function. In this particular problem, the initial guess is the *initial distribution* of the devices.

We start with distributing dampers by placing them to protect the undamped lower fundamental modes. Here, by assuming that only few of the lower modes contribute to the response in earthquake excitations, we use the 1^{st} and 2^{nd} modes. Evaluating these mode-shapes we can observe the floors with the largest differences. And by dividing each mode shape with the sum, the scaled factor can be obtained. With the sum of the two scaled factors, due to the fact we use the 1^{st} and 2^{nd} modes for each floor, we have a value that represents the contribution of each floor for the undamped or the modified system's response. However, we must point out that due to the fact that the 1^{st} and 2^{nd} modes do not contribute the same in the response, we use a participation factor Γ to identify the amount of contribution due to each mode. This is determined entirely upon the design engineer's intuition or by any other empirical way the design engineer might utilize. We then distribute the given amount of damping, total sum of the damping coefficients, by these values.

The floors which are filled with the devices are considered as *baskets*. The concept of

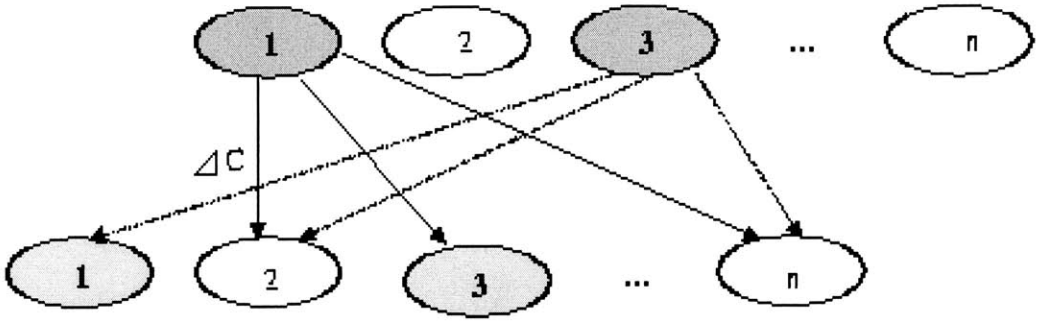

Figure 2-6: Basket Diagram

using baskets reduces the confusion between the iteration process throughout the search procedure. Assuming that the given MDOF system has n dof's, and that we have b baskets that contain dampers. The search iteration for the next step will cost only $b(n-1)$ times.

After the initial guess step, the actual search process begins. We first imply a constraint that the sum of the damping coefficients is constant. By taking a differential Δc from a basket and installing it back into another possible floor, we may obtain the gradient of the function which is consisted with the maximum amplitude of the transfer function. This is also the *sensitivity* of the function. Thus, by following the more sensitive path to the differential change, we are moving to our objective point in the n dimensional space; the minimum point. We may conceptually visualize this whole concept as a arbitrary line in $2D$, which is consisted with the maximum amplitudes of the transfer function of the structure. In such case the number of variables is 2, and thus, only 2 paths to follow. For an n MDOF system, the space is an n dimension, and n paths to follow.

Eventually, we are following the steepest curvature of the surface from an initial point, which was given by the initial guess, to the nadir, by varying the given variables (Fig. (2-7)). Ultimately, we consider the distribution of the damping coefficients as the strategic design.

2.3.3 Search Technique Process

The design process is:

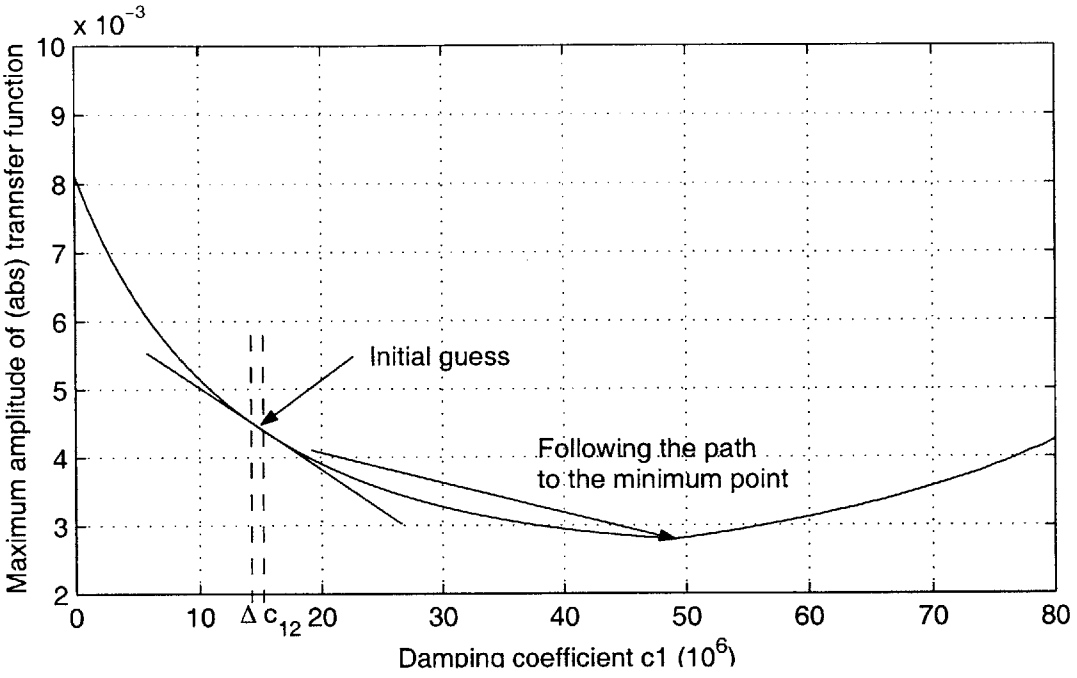

Figure 2-7: $2D$ case: $\sum c = \mathfrak{C}$ (Const)

Step 1. Initial Design Properties

- Given initial structural properties
- Define the sum of damping coefficients $\mathfrak{C}$
- Define structural/architectural constraints
- Define initial guess: Distribution of damping coefficients
- Define function $\mathcal{F} = \mathcal{F}(c_1, c_2, \ldots, c_n)$ which defines the maximum absolute amplitude of the transfer function

Step 2. Evaluate: $\mathfrak{g}_{ij} = -\partial\mathcal{F}/\partial\Delta c_{ij}$

Step 3. Search Technique

- Obtain the maximum gradient $\mathfrak{g}_{ij}$
- If $\mathfrak{g}_{ij} \geqslant 0$: take out Δc from c_i and re-install in c_j, and return to Step 2
- If $\mathfrak{g}_{ij} < 0$: end iteration

Step 4. Ultimate Design: Compare response with design criteria:

- If O.K: design is successful
- If N.G: return to Step 1 and redesign

However, we must note that due to the complexity of the function $mathcal F$, and the initial guess, during the search procedure the path might lead into a pit. By modifying Step 3 this obstacle could be overcomed.

2.3.4 Limitations

Although the search technique is a general approach, it posses several limitations when implemented.

The first is that in the numerical process the design criteria cannot be directly installed. This implies that the process must have an additional dynamic analysis step to obtain the response.

Second, the response of a structure is a combination of several modes. Which implies that other modes do contribute in the response. However, the search technique only has control over the maximum transfer function of a floor, which usually is obtained from the 1^{st} mode. Thus, while the process is minimizing the maximum transfer function of the floor, it could also be amplifying other modes. In such cases where the external excitation is distributed over a certain range of frequencies, the obtained results might not be preferable.

In addition to the previous limitations, implementing other design features, referred in Section 2.2.5, is not a simple task either

Chapter 3

Dynamic Analysis Tools

3.1 State space formula

We first start with the general equation of motion. Transferring the relative displacement to inter-story drifts would be a performed only in the real numerical examples later on.

$$m\ddot{u}(t) + c\dot{u}(t) + ku(t) = P(t) \tag{3.1}$$

We can easily formulate the state space formulation by introducing the state vector, $\mathbf{X}(t)$ which is a 2n-dimensional vector of the form,

$$\mathbf{X}(t) = \begin{bmatrix} \mathbf{u}(t) \\ \dot{\mathbf{u}}(t) \end{bmatrix} \tag{3.2}$$

Then we may express the motion of equation of a n-dimensional linear system in 2n-dimension general state space formulation,

$$\dot{\mathbf{X}}(t) = \mathbf{A}\mathbf{X}(t) + \mathbf{B}\mathbf{F}(t) + \mathbf{D}\mathbf{F_1}(t) \tag{3.3}$$

where, the state space coefficient matrices $\mathbf{A}$ and $\mathbf{B}$ are

$$\mathbf{A} = \begin{bmatrix} \mathbf{zeros(n)} & \mathbf{I(n)} \\ -\mathbf{M^{-1}K} & -\mathbf{M^{-1}C} \end{bmatrix}, \quad \mathbf{B} = \begin{bmatrix} \mathbf{zeros(n)} \\ \mathbf{M^{-1}E_f} \end{bmatrix} \quad \textit{and} \quad \mathbf{D} = \begin{bmatrix} \mathbf{zeros(n)} \\ \mathbf{M^{-1}E} \end{bmatrix} \tag{3.4}$$

$\mathbf{E_f}$ and $\mathbf{E}$ is the matrix which distributes the force matrices $\mathbf{F}$ and $\mathbf{F_1}$ along the structure. If this problem reduces to a passive control problem than the control matrix $\mathbf{D}$ vanishes. And we obtain the simplified general state space formulation.

3.2 Solution to $\dot{\mathbf{X}} = \mathbf{AX} + \mathbf{BF}$

We start with the unforced vibration problem,

$$\dot{\mathbf{X}} = \mathbf{AX} \tag{3.5}$$

We are familiar with this problem of dynamics, when we say $\mathbf{A} = a$ is a scalar, thus, the problem changes to a scalar differential equation. The solution can be expressed as $x = e^{at}x(0)$. Then, by an analytical argument we may show that the solution for Eqn. (3.5) is also in that form,

$$\mathbf{X}(t) = e^{At}x(0) \tag{3.6}$$

where, $\mathbf{X}$ is a $n*1$ matrix and e^{At} is a $n*n$ matrix. Now for the scalar differential equation problem it is known that

$$e^{at} = 1 + at + \frac{a^2t^2}{2!} + \frac{a^3t^3}{3!} + \cdots + \frac{a^kt^k}{k!} + \ldots \tag{3.7}$$

Therefore, a correct mathematical expression for e^{At} would also be in the form,

$$\mathbf{e^{At}} = \mathbf{I} + \mathbf{A}t + \frac{\mathbf{A}^2t^2}{2!} + \frac{\mathbf{A}^3t^3}{3!} + \cdots + \frac{\mathbf{A}^kt^k}{k!} + \ldots \tag{3.8}$$

Now we consider the force vibration problem. By following the same analytical argument from the scalar differential problem we may obtain the solution as

$$\mathbf{e^{-At}\dot{x}} = \mathbf{e^{-At}Ax} + \mathbf{e^{-At}BF} \tag{3.9}$$

and by recollecting the $\mathbf{x}$ terms on to the l.h.s.

$$\mathbf{e^{-At}\dot{x}} - \mathbf{e^{-At}Ax} = \mathbf{e^{-At}BF} \tag{3.10}$$

Now the left-hand side is exactly the derivative of $e^{-\mathbf{A}t}\mathbf{x}$, thus, we may rewrite Eqn. (3.10) as

$$\frac{d}{dt}\mathbf{e}^{\mathbf{A}t}\mathbf{x} = \mathbf{e}^{-\mathbf{A}t}\mathbf{B}\mathbf{F} \tag{3.11}$$

by integrating both sides we obtain,

$$\mathbf{e}^{-\mathbf{A}t}\mathbf{x} - \mathbf{e}^{-\mathbf{A}(0)}\mathbf{x}(0) = \int_0^t \mathbf{e}^{-\mathbf{A}\tau}\mathbf{B}\mathbf{F}(\tau)d\tau \tag{3.12}$$

and because $\mathbf{e}^{-\mathbf{A}(0)} = \mathbf{I}$

$$\mathbf{e}^{-\mathbf{A}t}\mathbf{x} = \mathbf{I}\mathbf{x}(0) + \int_0^t \mathbf{e}^{-\mathbf{A}\tau}\mathbf{B}\mathbf{F}(\tau)d\tau \tag{3.13}$$

Finally, we may obtain the general solution by premultipling both sides of the previous Eqn. by $\mathbf{e}^{\mathbf{A}t}$

$$\mathbf{x} = \mathbf{e}^{\mathbf{A}t}\mathbf{x}(0) + \mathbf{e}^{\mathbf{A}t}\int_0^t \mathbf{e}^{-\mathbf{A}\tau}\mathbf{B}\mathbf{F}(\tau)d\tau \tag{3.14}$$

Here, we will use a more commonly written form of the above Eqn.

$$\mathbf{x} = \mathbf{e}^{\mathbf{A}t}\mathbf{x}(0) + \int_0^t \mathbf{e}^{\mathbf{A}(\tau-t)}\mathbf{B}\mathbf{F}(\tau)d\tau \tag{3.15}$$

If $\mathbf{A}$ was a diagonal matrix than the $e^{\mathbf{A}t}$ term would have been exactly the same as taking the exponential of each element in $\mathbf{A}$. However, shown in Eqn. (3.4) matrix $\mathbf{A}$ is not diagonal so to make the computation more precise and concise we must transform the general state-space equation into a more efficient form.

3.3 Non-symmetric Eigenvalue Problem

To start with we first lay out the general Passive control state space equation which will be the main issue in this study.

$$\dot{\mathbf{X}}(t) = \mathbf{A}\mathbf{X}(t) + \mathbf{B}\mathbf{F}(t) \tag{3.16}$$

We first assume that $\mathbf{X}(t) = \mathbf{V}e^{\lambda t}$ is the solution for the standard eigenvalue problem $\dot{\mathbf{X}} = \mathbf{AX}$ and we get,

$$\mathbf{AV}_i = \lambda_i \mathbf{V}_i \quad i = 1, 2, \ldots, 2n \tag{3.17}$$

where, λ_i and V_i are eigenvalues and eigenvectors of $\mathbf{A}$. We must point out that the $\mathbf{A}$ matrix is not symmetric. This induces the eigenvalues and eigenvectors, in general, to be both complex, and lose it's orthogonality. However, by introducing the adjoint eigenvalue problem

$$\mathbf{A}^T \mathbf{W}_j = \lambda_j \mathbf{W}_j \quad j = 1, 2, \ldots, 2n \tag{3.18}$$

we may obtain another orthogonal property. In general, $\mathbf{V}$ is referred as the right eigenvector and $\mathbf{W}$ as the left eigenvector. These vectors satisfy the biorthogonality property, that is

$$\mathbf{W}_j^T \mathbf{V}_i = \alpha_i \delta_{ij} \quad \delta_{ij} = \textit{Kronecker delta} \tag{3.19}$$

where, δ_{ij} is the *Kronecker delta.* Where, α is the product of the right and left eigenvectors that possesses the same eigenvalues. We may also normalize the length of $\mathbf{W}_j$ and $\mathbf{V}_j$ to unity. This problem also possesses the biorthoganlity with respect to the matrix $\mathbf{A}$.

$$\mathbf{W}_j^T \mathbf{AV}_i = \lambda_i \alpha_i \delta_i \quad i, j = 1, 2, \ldots, 2n \tag{3.20}$$

Now, that we have Eqn. (3.20), we assume,

$$\mathbf{X}(t) = \mathbf{Vq}(t) \tag{3.21}$$

and insert this back into equation Eqn. (3.16).

$$\mathbf{V}\dot{\mathbf{q}}(t) = \mathbf{AVq}(t) + \mathbf{BF}(t) \tag{3.22}$$

and if we premultiply this by $\mathbf{W^T}$ due to the biorthogonality, we may obtain the uncoupled set of equations

$$\mathbf{W}^T\mathbf{V}\dot{\mathbf{q}}(t) = \mathbf{W}^T\mathbf{A}\mathbf{V}\mathbf{q}(t) + \mathbf{W}^T\mathbf{B}\mathbf{F}(t) \tag{3.23}$$

$$\alpha\dot{\mathbf{q}}(t) = \alpha\Lambda\mathbf{q}(t) + \mathbf{W}^T\mathbf{B}\mathbf{F}(t) \tag{3.24}$$

where,

$$\alpha = \text{diag}[\alpha_1, \alpha_2, \ldots, \alpha_{2n}] \tag{3.25}$$

$$\mathbf{q}^T = [q_1, q_2, \ldots, q_{2n}] \tag{3.26}$$

$$\Lambda = \text{diag}[\lambda_1, \lambda_2, \ldots, \lambda_{2n}] \tag{3.27}$$

And it is shown that both α and Λ exist as complex diagonal matrices. In addition, the product $\mathbf{W}^T\mathbf{B}\mathbf{F}(t)$ is a vector, thus we have decomposed Eqn. (3.24) into a 2n independent 1^{st} order differential equation, with the solution vector $q(t)$ in the complex domain. This is however, conceptually not easy to visualize due to the fact that we are dealing with complex variables in the time domain.

3.3.1 Transform of State-space

We first start with the decoupled formulation given in Eqn. (3.24) in Section 3.3.

$$\alpha_i\dot{q}_i = \alpha_i\lambda_i q_i + \mathbf{W}^T\mathbf{B}\mathbf{F} \qquad i = 1, 2, \ldots, 2n \tag{3.28}$$

And it is proven **reference** that both α and Λ exist as complex conjugate pairs. Notice that the modal forces $\mathbf{W}_i^T\mathbf{B}\mathbf{F}(t)/\alpha_i$ appears in complex conjugate pairs as well. Thus, we may separate the conjugates pairs and rewrite Eqn. (3.28) as follows

$$\dot{q}_i = \lambda_i q_i + f_i \qquad i = 1, 2, \ldots, n \tag{3.29}$$

$$\dot{\tilde{q}}_i = \tilde{\lambda}_i\tilde{q}_i + \tilde{f}_i \qquad i = 1, 2, \ldots, n \tag{3.30}$$

where,

$$f_i = \mathbf{W}_i\mathbf{B}\mathbf{F}/\alpha_i \qquad i = 1, 2, \ldots, n \tag{3.31}$$

and $\tilde{f}_i$ is the conjugate pair of f_i. As mentioned before α, λ and f are all in the complex plane. So we now transform the equation to the real coordinates by using the conjugate pair properties. Eqn. (3.29) may be rewritten in the form,

$$\dot{q}_R + i\dot{q}_I = (\lambda_R + i\lambda_I)(q_R + iq_I) + (f_R + f_I) \tag{3.32}$$

$$\dot{q}_R - i\dot{q}_I = (\lambda_R - i\lambda_I)(q_R - iq_I) + (f_R - f_I) \tag{3.33}$$

by summing and subtracting Eqn. (3.32) and Eqn. (3.33) we obtain

$$\dot{q}_R = \lambda_R q_R - \lambda_I q_I + f_R \tag{3.34}$$

$$\dot{q}_I = \lambda_I q_R + \lambda_R q_I + f_I \tag{3.35}$$

and we may rewrite Eqn. (3.34) and Eqn. (3.35) in matrix formulation,

$$\begin{bmatrix} \dot{q}_R \\ \dot{q}_I \end{bmatrix} = \begin{bmatrix} \lambda_R & -\lambda_I \\ \lambda_I & \lambda_R \end{bmatrix} \begin{bmatrix} q_R \\ q_I \end{bmatrix} + \begin{bmatrix} f_R \\ f_I \end{bmatrix} \tag{3.36}$$

Now, the solution may be obtained by the general state-space solution stated previously in Section 3.2. We should point out that even if we lay out the form in global coordinates the state-space coefficient matrix Λ will be in a sparse matrix (banded) formation such as,

$$\Lambda_T = \begin{bmatrix} \Lambda_{T1} & & & \mathbf{0} \\ & \Lambda_{T2} & & \\ & & \ddots & \\ \mathbf{0} & & & \Lambda_{Tn} \end{bmatrix} \tag{3.37}$$

We may point out that now we need not have to deal with the global $2n * 2n$ matrix but just the joint $2 * 2$ matrix. However, using the general solution to the state-space approach is not trivial. In addition due to the fact that Λ is not diagonal, the result is an approximate. Various solution methods have been proposed to solve this with numerical efficiency. However, applying the frequency analysis may obtain a efficient and accurate dynamic analysis.

3.4 Frequency Domain Analysis

We again start with the previous derived Eqn. (3.34) and Eqn. (3.35) for a joint.

$$\dot{\mathbf{q}}_T = \Lambda_T \mathbf{q}_T + \mathbf{f}_T \tag{3.38}$$

where,

$$\mathbf{q}_T = \begin{bmatrix} q_R \\ q_I \end{bmatrix}, \Lambda_T = \begin{bmatrix} \lambda_R & -\lambda_I \\ \lambda_I & \lambda_R \end{bmatrix} \text{ and } \mathbf{f}_T = \begin{bmatrix} f_R \\ f_I \end{bmatrix} \tag{3.39}$$

We transform the forces f_R and f_I into the frequency domain by expressing them as summations of harmonic functions of different frequencies. The transformation of the forcing terms are represented as the following,

$$F_j(\omega) = \int_{-\infty}^{\infty} f_j(t) e^{-i\omega t} dt \quad j = 1, 2, \ldots, n \tag{3.40}$$

while, the response is in the inverse Fourier transform,

$$q_j(t) = \frac{1}{2\pi} \int_{-\infty}^{\infty} H_j(\omega) F_j(\omega) e^{i\omega t} d\omega \quad j = 1, 2, \ldots, n \tag{3.41}$$

To obtain the response in the frequency domain we must also form the complex transfer function $\mathbf{H}(\omega)$. Thus, if Eqn. (3.38) is Fourier transformed, we have

$$(i\omega \mathbf{I} - \Lambda_{Ti}) \bar{\mathbf{q}}_{Ti} = \bar{\mathbf{f}}_{Ti} \qquad i = 1, 2, \ldots, n \tag{3.42}$$

Here, we note that $\bar{\mathbf{q}}$ is also the Fourier transform of $\mathbf{q}$. We then may express $(i\omega \mathbf{I} - \Lambda)$ as $\bar{K}_{Ti}$ and follow on to the next expression

$$\bar{\mathbf{q}}_{Ti} = \bar{\mathbf{K}}_{Ti}^{-1} \bar{\mathbf{f}}_{Ti} = \mathbf{H}_{Ti} \bar{\mathbf{F}}_{Ti} \tag{3.43}$$

where, $\mathbf{H}$ is the complex transfer function. After the frequency domain response is obtained the inverse Fourier transform is executed to reevaluate the response in time domain. From a physical point of view, $\mathbf{X}(t)$ is to be real throughout the time domain. Thus, V_i and q_i must appear in conjugate pairs in order to keep the response in the real axis.

Accommodating the conjugate pairs we obtain,

$$X(t) = \sum_{i=1}^{n} V_i q_i(t) + \tilde{V}_i \tilde{q}_i(t) \tag{3.44}$$

Thus, we can reorganize the previous equation as,

$$\begin{aligned} \sum_{i=1}^{n} V_i q_i(t) + \tilde{V}_i \tilde{q}_i(t) &= \sum_{i=1}^{n} \Big[(V_{iR} + iV_{iI})(q_{iR} + iq_{iI}) + (V_{iR} - iV_{iI})(q_{iR} - iq_{iI}) \Big] \\ &= 2 \sum_{i=1}^{n} (V_{iR} q_{iR}(t) - V_{iI} q_{iI}(t)) \end{aligned} \tag{3.45}$$

We have finally obtained the response, i,e., the inter-story drift and inter-story velocity, of the structure.

3.4.1 FFT and IFFT

As mentioned in the previous Section, we integrate from the *time* domain to the *frequency* domain, and back to obtain the response of the structure. Due to discrete-time signals of earthquakes, and the fact that computers are inputed with discrete digital data, the actual Fourier transform must be in discrete form. Thus, the continuous form of Eqn. (3.40) and Eqn. (3.41) can both be rewritten in a discrete form as,

$$F_{jk} = \frac{1}{N} \sum_{m=0}^{N-1} f_{jm} e^{-i\frac{2\pi km}{N}} \qquad k = 0, 1, \ldots, N-1 \tag{3.46}$$

$$q_{jm} = \sum_{k=0}^{N-1} H_{jk} F_{jk} e^{i\frac{2\pi km}{N}} \qquad m = 0, 1, \ldots, N-1 \tag{3.47}$$

We may notice that the only differences between the two transforms are the change of sign in the exponential term and the dividing factor N in the response. Such that one algorithm can be obtained with just a slight modification of the other.

Conventional discrete Fourier transforms needed $O(N^2)$ operations in the process. However, the proposed algorithm by Danielson and Lanczos in 1942 i.e., Danielson-Lanczos Lemma, reduced the process to $O(N \log_2 N)$. This lemma showed that a discrete Fourier transform of length N can be represented with 2 copies of a Fourier transform of the length

of $N/2$.

$$\mathfrak{F}_n = \begin{bmatrix} \mathbf{I} & \mathbf{D} \\ \mathbf{I} & -\mathbf{D} \end{bmatrix} \begin{bmatrix} \mathfrak{F}_{n/2} & \mathbf{0} \\ \mathbf{0} & \mathfrak{F}_{n/2} \end{bmatrix} \begin{bmatrix} \mathfrak{O} \end{bmatrix} \tag{3.48}$$

where, $\mathfrak{F}$ is defined in [9], as the *Fourier Matrix*

$$\mathfrak{F}_n = \begin{bmatrix} 1 & 1 & 1 & . & 1 \\ 1 & w & w^2 & . & w(n-1) \\ 1 & w^2 & w^4 & . & w^{2(n-1)} \\ . & . & . & . & . \\ 1 & x^{n-1} & w^{2(n-2)} & . & w^{(n-1)^2} \end{bmatrix} \tag{3.49}$$

where, w is

$$w = e^{\frac{2\pi i}{N}}, \qquad \textit{and} \qquad w^n = e^{2\pi i} = 1 \tag{3.50}$$

and, $\mathbf{I}$ is a $n/2 * n/2$ Identical matrix, and

$$\mathbf{D} = \begin{bmatrix} i^0 & 0 & 0 & \dots & 0 \\ 0 & i^1 & 0 & \dots & 0 \\ 0 & 0 & i^2 & \dots & 0 \\ \vdots & \vdots & \vdots & \ddots & 0 \\ 0 & 0 & 0 & 0 & i^{n/2} \end{bmatrix} \tag{3.51}$$

$\mathfrak{O}$ is a matrix that reorganizes the even and odd functions, such for a $4 * 4$ matrix for an example, it would look like,

$$\begin{bmatrix} x_{even} \\ x_{odd} \end{bmatrix} = \begin{bmatrix} 1 & 0 & 0 & 0 \\ 0 & 0 & 1 & 0 \\ 0 & 1 & 0 & 0 \\ 0 & 0 & 0 & 1 \end{bmatrix} \begin{bmatrix} x_0 \\ x_1 \\ x_2 \\ x_3 \end{bmatrix} = \begin{bmatrix} \mathfrak{O} \end{bmatrix} \begin{bmatrix} x \end{bmatrix} \tag{3.52}$$

The fundamental concept which the FFT is based on is the connection between, $\mathfrak{F}_N$ and $\mathfrak{F}_{N/2}$. And by using the *bit reversal* we can determine the input and output relationship.

This is better explained with Fig. (3.4.1).

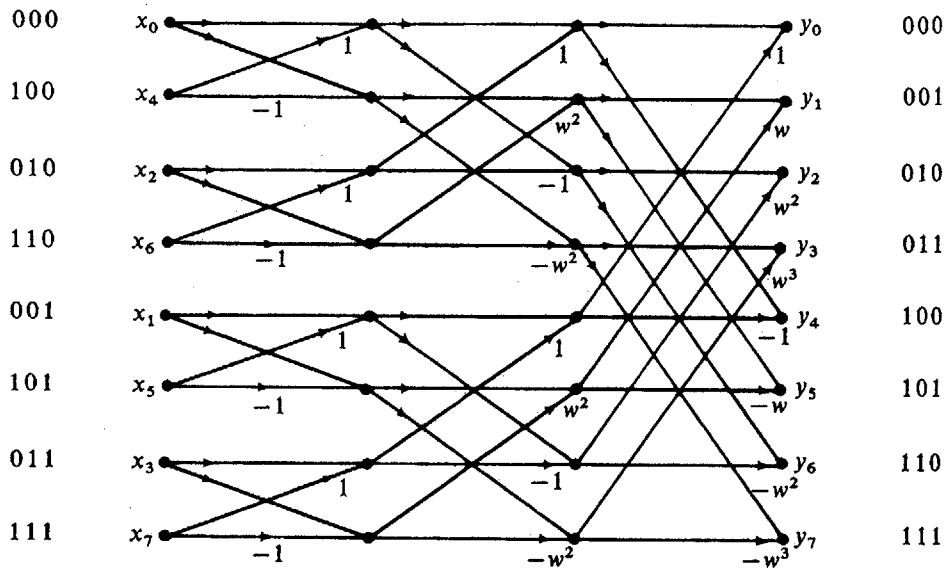

Figure 3-1: Butterfly flow chart

It shows the order that the nx's enter the FFT and the stages that take them through, and the simplicity of the logic. The rule for the permutation of x's before entering the FFT, is to write the subscripts in binary and reverse the order of their bits. The subscripts appear in *bit reversed order* on the left side of the graph.

The speed of the FFT depends on working with highly composite numbers, having many factors; for a prime number this factorizing concept may not be applicable such that a completely different algorithm is necessary. However, most codes allow any factors, here to concentrate on the relation between $\mathfrak{F}_N$ and $\mathfrak{F}_{N/2}$ we assumed it to be in a power of 2. While we can express $\mathfrak{F}_N$ with $\mathfrak{F}_{N/2}$ this connection can go all the way to the factor of 1, such as $\mathfrak{F}_1$. Thus, the sparse matrix multiplications will eventually reduce the whole computation to $O(N \log_2 N)$.

However, in this study due to the fact that we had obtained the complex transfer function directly, and not by the Fourier transform, we must make mirror images of the complex transfer function to complete Eqn. (3.47). Such that the complex transfer functions are mirrored with respect to $H_{N/2+1}$ in the middle. This gives,

$$\mathbf{H}_{1+i} = \mathbf{H}_{N+1-i} \quad i = 1, 2, \ldots, N/2 \tag{3.53}$$

We point out that the complex transfer function is composed with n numbers of $\mathbf{H_{Ti}}$, *joint* $2 * 2$ matrices, which eventually gives a $2n * 2n$ matrix. And by careful inspections, we do not need all, but only one of each conjugate eigenvalue pairs for the complex transfer functions.

Wrap-around Effect

However, due to the presumption of the basic Fourier transform algorithm, there exist some numerical and physical problems. The first problem deals with the length of the input data. As earthquake inputs are arbitrary, for the input length of the input data to be exactly in order of 2 is impossible. The other problem is due to the presumption that the excitation is a periodic function, thus, letting us cut the infinite integral into a finite summation. If the response of the excitation has not died out after the length of FFT, the response near the beginning will be influenced by the end excitation. These problems invoke when there is not enough time for the response of the previous period of the excitation is allowed to die out before the new one comes in. This is called the *wrap-around effect.* To solve this problem previous studies have used the simple *zero padding* technique, however, here we use a more sophisticated technique which has been largely used in digital signal processing, called the *Exponential Window Method.*

3.4.2 Exponential Window Method

While FFT is an attractive and widely used solution for dynamic problems. It is also necessary to add at the end of the force history a quiet zone, which is consisted with trailing zeros. However, the duration of this trailing of zeros must allow the free vibration to damp out and reach a desired tolerance. The duration of this zone to meet the desired performance is a function of the fundamental period of the system and also the amount of damping inside the system. However, the time and cost of computation may become impractical. To overcome these difficulties we use a tool commonly used in digital signal processing, the *exponential window method* (EWM). Kausel et al [7] evaluated the accuracy

and efficiency when applied to civil engineering and structural dynamics analysis. Here, we apply it to our dynamic analysis model, the state-space formula.

Application to State-space formula

We have already arrived to the response equation in the frequency domain in Eqn. (3.43). The inverse transform is

$$\mathbf{q}_{Ti}(t) = \frac{1}{2\pi}\int_{-\infty}^{\infty} \mathbf{H}_{Ti}(i\omega)\bar{\mathbf{F}}_{Ti}(\omega)e^{i\omega t}d\omega \tag{3.54}$$

where, $\bar{F}(\omega)$ is the fourier transform of the causel excitation $f(t)$, and $H(\omega)$ is the transfer function in frequency domain. The equation can be evaluated by contour integration,

$$\mathbf{q}_{Ti}(t) = \frac{1}{2\pi}\oint \mathbf{H}_{Ti}(z)\bar{\mathbf{F}}_{Ti}(z)e^{izt}dz \tag{3.55}$$

where, z is the complex frequency. Here, an arbitrary downward shift a of the integration path can be executed, while obtaining the same result [7]. For $t > 0$, Eqn. (3.55) can be rewritten in the form,

$$\mathbf{q}_{Ti}(t) = \frac{1}{2\pi}\int_{-\infty}^{\infty} \mathbf{H}_{Ti}(\omega - ia)\bar{\mathbf{F}}_{Ti}(\omega - ia)e^{i(\omega - ia)t}d\omega \tag{3.56}$$

Since, a is independent of ω,

$$\mathbf{q}_{Ti}(t) = e^{at}\frac{1}{2\pi}\int_{-\infty}^{\infty} \mathbf{H}_{Ti}(\omega - ia)\bar{\mathbf{F}}_{Ti}(\omega - ia)e^{i\omega t}d\omega = e^{at}\hat{\mathbf{q}}_{Ti}(t) \tag{3.57}$$

with,

$$\bar{\mathbf{F}}_{Ti}(\omega - ia) = \int_0^{t_d}[e^{-at}\mathbf{f}_{Ti}(t)]e^{-i\omega t}dt = \int_0^{t_d}\hat{\mathbf{f}}(t)e^{-i\omega t}dt \tag{3.58}$$

where, t_d is the duration time of the excitation. Now, we can observe that all we have done is obtained the solution for the system,

$$(iz\mathbf{I} - \bar{\Lambda}_{Ti})\bar{\mathbf{q}}_{Ti} = \bar{\mathbf{f}}_{Ti} \qquad i = 1, 2, \ldots, n \tag{3.59}$$

where, z is substituted by $\omega - ia$. It is hard to visualize the effect of the exponential window method in the state-space formulation. It could be implemented such that the exponential term kills out the error obtained by the periodic characteristic of the FFT. However, in the general dynamic equilibrium equation in the frequency domain, it can be visualized as a shift of the resonant frequencies from ω_i to $\sqrt{\omega_i^2 + a^2}$, and the present of an apparent fraction of critical damping $a/\sqrt{\omega_i^2 + a^2}$. Eventually, the exponential term in Eqn. (3.57) removes this equivalent damping effect. Thus, the response $\mathbf{q(t)}$ is the response.

Decision on arbitrary shift a

To implement the exponential window method successfully, an upper limit constraint on the arbitrary shifting constant a must be enforced. This is due to either loss of numerical precision, or underflows and overflows during the evaluation process. Kausel [7] presented an upper limit that depends on the precision with which the computations are made.

$$a < \frac{m \ln 10}{T} = m\Delta f \ln 10 \tag{3.60}$$

where, Δf is defined as the frequency step (sampling rate). In this study we used,

$$a = d\omega = 2\pi df \tag{3.61}$$

where, $d\omega$ is the frequency step in radian.

3.5 Impulse Response

The previous models were composed with the global structure for the formulation of the matrices. Here, we introduce a F.E.M model which does not require the construction and manipulation of large matrices. This will lead us to the transfer function that relates the response from the impulse load applied from the ground acceleration to the building response.

3.5.1 Seismic Excitation Model

We first start by denoting u_j and v_j as the displacement of the j^{th} floor and the resultant shear force in the columns of the j^{th} floor, respectively. The equation of motion and the

force-displacement relationship of the j^{th} floor will then be

$$V_j = V_{j-1} + m_j \ddot{u}_j \tag{3.62}$$

$$V_{j-1} = k_j(u_j - u_{j-1}) + c_j(\dot{u}_j - \dot{u}_{j-1}) \tag{3.63}$$

where, m_j, k_j and c_j are the mass, stiffness and damping coefficients of the j^{th} floor. In the frequency domain,

$$\bar{V}_j = \bar{V}_{j-1} - m_j\omega^2\bar{U}_j \tag{3.64}$$

$$\bar{V}_{j-1} = (k_j + ic_j\omega)\bar{U}_j - (k_j + ic_j\omega)\bar{U}_{j-1} \tag{3.65}$$

where, $\bar{V}$ and $\bar{U}$ are the *Fourier transforms* of V and u, respectively. Therefore,

$$\begin{bmatrix} \bar{U}_j \\ \bar{V}_j \end{bmatrix} = \begin{bmatrix} 1 & 1/(k_j + ic_j\omega) \\ -m_j\omega^2 & 1 - m_j\omega^2/(k_j + ic_j\omega) \end{bmatrix} \begin{bmatrix} \bar{U}_{j-1} \\ \bar{V}_{j-1} \end{bmatrix} \tag{3.66}$$

which can be condensed to

$$\mathbf{z}_j = \mathbf{T}_j\mathbf{z}_{j-1} \tag{3.67}$$

In the case for seismic excitation, the first floor transfer function is given as,

$$\begin{bmatrix} \bar{U}_1 \\ \bar{V}_1 \end{bmatrix} = \begin{bmatrix} 1/\omega^2 & 1/(k_1 + ic_1\omega) \\ -m_1 & 1 - m_1\omega^2/(k_1 + ic_1\omega) \end{bmatrix} \begin{bmatrix} \ddot{\bar{U}}_0 \\ \bar{V}_0 \end{bmatrix} \tag{3.68}$$

or,

$$\mathbf{z}_1 = \mathbf{T}_1\mathbf{z}_0 \tag{3.69}$$

were $\ddot{\bar{U}}_0$ is the fourier transform of the ground acceleration. Now the general expression is

$$\mathbf{z}_l = \mathbf{T}_l\mathbf{T}_{l-1}, \ldots, \mathbf{T}_1\mathbf{z}_0 \tag{3.70}$$

Boundary conditions are employed to find the response at each floor,Say $\ddot{\bar{U}}_0$ be the Dirac delta function, so its fourier transform is unity. Then the responses are the impulse response

function, and their Fourier transforms, represented by the state vector $\mathbf{z}_j$, are the frequency response functions. Thus

$$\mathbf{Z}_N = \begin{bmatrix} \bar{U}_N \\ 0 \end{bmatrix} \tag{3.71}$$

$$\mathbf{Z}_O = \begin{bmatrix} 1 \\ \bar{V}_0 \end{bmatrix} \tag{3.72}$$

Substituting Eqn. (3.71) and Eqn. (3.72) into Eqn. (3.70)

$$\begin{bmatrix} \bar{U}_N \\ 0 \end{bmatrix} = \begin{bmatrix} b_{11} & b_{12} \\ b_{21} & b_{22} \end{bmatrix} \begin{bmatrix} 1 \\ \bar{V}_0 \end{bmatrix} = \mathbf{B} \begin{bmatrix} 1 \\ \bar{V}_0 \end{bmatrix} \tag{3.73}$$

where we may find the two unknowns,

$$\bar{V}_0 = \frac{-b_{12}}{b_{22}} \tag{3.74}$$

$$\bar{U}_2 = b_{11} - \frac{b_{12}b_{21}}{b_{22}} \tag{3.75}$$

Now that we have obtained the two unknowns that identify the response, the response of the structure under a unit impulse is obtained. However, having the inter-story strain as our design criteria, we formulate the response by inter-story drifts.

$$u_1 = v_1 \tag{3.76}$$

$$u_n - u_{n-1} = v_n \tag{3.77}$$

where, v_n denotes the inter-story drift of the j^{th} floor. However, when expressed by the state vector the previous equation becomes,

$$\mathbf{z}_1 = \mathbf{v}_1 \tag{3.78}$$

$$\mathbf{z}_n - \mathbf{z}_{n-1} = \mathbf{v}_n \tag{3.79}$$

which becomes,

$$\mathbf{v}_1 = \mathbf{z}_1 \tag{3.80}$$

$$\mathbf{v}_n = (\mathbf{T}_n - \mathbf{I})\mathbf{z}_{n-1} \tag{3.81}$$

The obtained response is thus the transfer function of the systems due to an impulse excitation applied by a ground acceleration. The amplitudes of these values; the amplitudes of the transfer functions, will be later minimized in order to mitigate the vibration due to earthquake excitation.

Now we may proceed to find the statistics of the response due to an earthquake excitation. The earthquake ground acceleration has often been modeled as a stationary stochastic process with a zero mean and a power spectral density function $S_{\ddot{u}_g}$. We can now find the mean square response σ_m^2 of the structure at each floor by,

$$\sigma_m^2 = \int_{-\infty}^{\infty} |Z_m|^2 S_{\ddot{u}_g} d\omega, \qquad m = 1, 2, \ldots, N \tag{3.82}$$

If the external excitation is modeled as a stationary random process characterized by its power spectral density function (PSDF), then the PSDF of the responses of the structural system is given by

$$S_u(\omega) = |Z(i\omega)|^2 S_{\ddot{u}_g}(i\omega) \tag{3.83}$$

where $S_{\ddot{u}_g}(i\omega)$ is the PSDF of the excitation of the acceleration, $\ddot{u}_g$. Now, for the inter-story drift

$$v_i(t) = u_i(t) \quad for \quad i = 1 \tag{3.84}$$

$$v_i(t) = u_i(t) - u_{i-1}(t) \quad for \quad i = 2, 3, \ldots, N \tag{3.85}$$

where, $v(t)$ is vector of inter-story drift. PSDF of inter-story drift $S_x(\omega)$ is given as,

$$S_{x_i}(\omega) = S_{u_i}(\omega) \quad for \quad i = 1 \tag{3.86}$$

$$S_{x_i}(\omega) = S_{u_i}(\omega) - S_{u_i u_{i-1}}(i\omega) - S_{u_{i-1} u_i}(i\omega) + S_{u-1_i}(\omega)$$
$$for \quad i = 2, 3, \ldots, N \tag{3.87}$$

where, $S_{u_i u_{i-1}}(\omega)$ and $S_{u_{i-1} u_i}(\omega)$ are cross PSDFs between story displacements of the building frame and are given as

$$S_{u_i u_{i-1}}(i\omega) = Z_i^*(\omega) Z_{i-1}(\omega) S_{\ddot{u}_g}(\omega) \tag{3.88}$$

$$S_{u_{i-1} u_i}(i\omega) = Z_{i-1}^*(\omega) Z_i(\omega) S_{\ddot{u}_g}(\omega) \tag{3.89}$$

$$\tag{3.90}$$

3.5.2 Wind Excitation Model

The wind excitation model can be directly derived from the seismic model, with only a few changes. Let us use the same denotations as before while just adding a external force term, $P_j(t)$ applied on the j^{th} floor. The equation of motion and the force-displacement relationship of the j^{th} floor are

$$V_j = V_{j-1} + m_j \ddot{u}_j - P_j \tag{3.91}$$

$$V_{j-1} = k_j(u_j - u_{j-1}) + c_j(\dot{u}_j - \dot{u}_{j-1}) \tag{3.92}$$

Then by taking the Fourier transform as before,

$$\bar{V}_j = \bar{V}_{j-1} - m_j \omega^2 \bar{U}_j - \bar{P}_j \tag{3.93}$$

$$\bar{V}_{j-1} = (k_j + i c_j \omega)\bar{U}_j - (k_j + i c_j \omega)\bar{U}_{j-1} \tag{3.94}$$

where, now $\bar{P}_j$ is the Fourier transforms of P_j. Therefore,

$$\begin{bmatrix} \bar{U}_j \\ \bar{V}_j \end{bmatrix} = \begin{bmatrix} 1 & 1/(k_j + i c_j \omega) \\ -m_j \omega^2 & 1 - m_j \omega^2/(k_j + i c_j \omega) \end{bmatrix} \begin{bmatrix} \bar{U}_{j-1} \\ \bar{V}_{j-1} \end{bmatrix} - \begin{bmatrix} 0 \\ \bar{P}_j \end{bmatrix} \tag{3.95}$$

which can than be layed out as

$$\mathbf{z}_1 = \mathbf{T}_1\mathbf{z}_0 - \mathbf{P}_1 \tag{3.96}$$

$$\mathbf{z}_2 = \mathbf{T}_2\mathbf{T}_1\mathbf{z}_0 - \mathbf{T}_2\mathbf{P}_1 - \mathbf{P}_2 \tag{3.97}$$

$$\vdots \qquad \vdots \qquad \vdots$$

$$\mathbf{z}_L = \mathbf{T}_L\mathbf{T}_{L-1}\ldots\mathbf{T}_1\mathbf{z}_0 - (\mathbf{T}_L\mathbf{T}_{L-1}\ldots\mathbf{T}_2\mathbf{P}_1 + \mathbf{T}_L\mathbf{T}_{L-1}\ldots\mathbf{T}_3\mathbf{P}_2 + \cdots + \mathbf{T}_L\mathbf{T}_{L-1}\mathbf{P}_L + \mathbf{T}_L\mathbf{P}_{L-1} + \mathbf{P}_L) \tag{3.98}$$

So we may express the general equation as,

$$\mathbf{z}_L = \mathbf{T}_L\mathbf{T}_{L-1}\ldots\mathbf{T}_1\mathbf{z}_0 - \left[\sum_{i=1}^{L}\mathbf{T}_L\mathbf{T}_{L-1}\ldots\mathbf{T}_{i+1}\mathbf{P}_i\right] \tag{3.99}$$

In the case for wind excitation the ground displacement and the shear force on the top are both 0.

$$\mathbf{Z}_N = \begin{bmatrix}\bar{U}_N \\ 0\end{bmatrix} \tag{3.100}$$

$$\mathbf{Z}_O = \begin{bmatrix}0 \\ \bar{V}_0\end{bmatrix} \tag{3.101}$$

Substituting Eqn. (3.100) and Eqn. (3.101) into Eqn. (3.99)

$$\begin{bmatrix}\bar{U}_N \\ 0\end{bmatrix} = \begin{bmatrix}b_{11} & b_{12} \\ b_{21} & b_{22}\end{bmatrix}\begin{bmatrix}0 \\ \bar{V}_0\end{bmatrix} - \begin{bmatrix}P_{N1} \\ P_{N2}\end{bmatrix} \tag{3.102}$$

where we may find the two unknowns,

$$\bar{V}_0 = \frac{P_{N2}}{b_{22}} \tag{3.103}$$

$$\bar{U}_N = \frac{b_{12}P_{N2}}{b_{22}} - P_{N1} \tag{3.104}$$

Chapter 4

Evaluation and Comparison

In the previous Sections, the design concept, dynamic analysis tools, have been introduced. Now, we move on to the implementation of the study to various case studies. Here, we use 7 cases to evaluate and compare the proposed design concepts.

Structural Properties: case 1 - 7 $(M = kg * 1000, K = kN/cm)$

		1	2	3	4	5	6	7	8	9	10
case 1	M	600	600	550	500	500	350	350	275	200	200
	K	8000	8000	7000	6000	6000	4000	4000	3000	2000	2000
case 2	M	412.5	412.5	412.5	412.5	412.5	412.5	412.5	412.5	412.5	412.5
	K	5000	5000	5000	5000	5000	5000	5000	5000	5000	5000
case 3	M	550	550	550	550	550	275	275	275	275	275
	K	6300	6300	6300	6300	6300	2700	2700	2700	2700	2700
case 4	M	600	600	550	500	500	350	350	275	200	200
	K	11000	9500	7800	6500	5010	3820	2830	1830	1110	600
case 5	M	600	600	550	500	500	350	350	275	200	200
	K	9900	8550	7020	5850	4509	3438	2547	1647	999	540
case 6	M	80	80	80	80	80	80				
	K	400	400	400	400	400	400				
case 7	M	80	80	80	80	80	80				
	K	513.1	481	426	347.6	244.4	110				

Table 4.1: Structural Properties: case 1 - 7

The properties of the structures are given in Table. (4.1) The first case is the structure used in [10]. We then take various stiffness and mass distributions to evaluate. All the cases have the same amount of stiffness and mass coefficients, however, they differ by the distribution throughout the structure. Case 2 has both parameters uniformly distributed. Case 3 divided the structure in 2, and case 4 rearranged the stiffness in order to obtain a uniformly distributed 1^{st} mode. And by reducing 11% of stiffness of case 4, we have case 5.

Case 6, and 7 is the case study used in [13]. Here, too the two models only differ in the distribution of stiffness. The latter aiming for an uniform distribution of the amplitudes of transfer functions of inter-story drifts. In this study they are used to compare the results obtained by the *search technique.*

Here, we must also define the 4 external design excitations;

- Taft 1: Taft Lincoln School Tunnel (Comp N21E)
- Taft 2: Taft Lincoln School Tunnel (Comp S69E)
- El-Centro 1: El-Centro Site Imperial Valley Irrigation District (Comp S00E)
- El-Centro 2: El-Centro Site Imperial Valley Irrigation District (Comp S90W)

4.1 Simulation Design

The actual design is capable once the excitation, structural properties, and design constraints are provided.

The constraints on the structure is to restrict the inter-story strain within a given criteria. The imposed criteria is 1/200, thus, when the height of the floor of a structure is uniformly assumed as $4m$, we can directly convert it to a constraint on the inter-story drift, which would be $2cm$ for each floor.

We start with assigning Δc_j as a equivalent to a passive energy dissipation device in the i^{th} floor. Thus,

$$c_i = \sum_{j=1}^{m} \Delta c_j \tag{4.1}$$

Thus, c_i indicates the damping coefficient, and m indicates the number of dampers installed in i^{th} floor. The unit for a device is taken as $10^4 kNs/cm$. In addition to a constraint on

the inter-story strain, we can apply a constraint on the total number of devices allowed on a given floor, A/F, by controlling m.

In this study, we identify designs by writing the method's name first, followed by the A/F constraint, for an example, MID (15).

4.1.1 Design Evaluation: Case 1

The constraints imposed are:

- Target inter-story strain: $0.02(m)$
- Available Damper per floor (A/F): 20
- Total number of dampers (Tot): 80

With these constraints specified in the design, the strategic indices are evaluated. Fig. (4-1)

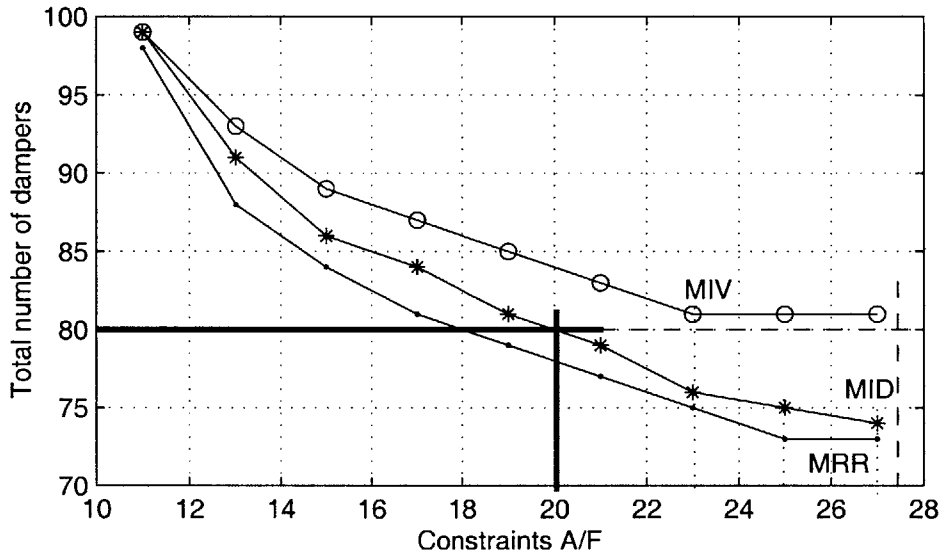

Figure 4-1: Design evaluation: Case 1

illustrates the comparison of the proposed methods. In case 1 the MRR index proves to be the most preferable. It also shows limitations of the indices. For the MIV index, the limit is 23 A/F. This is the first index that falls to the limit. The next index is the MRR, with 25 A/F followed with MID with 27 A/F. It shows that ignoring any cost/design constraints imposed on the problem, the MRR method eventually gives the optimal design with 73 total dampers installed.

If the A/F and Tot constraints are imposed the optimal design is given inside the squared area. In this case, MID (20) and MRR(19,20) designs are available. Thus, the MRR (20) design is the optimal design for case 1, with 78 total dampers installed.

Case 1: 80 Tot, 20 A/F

		Init. Values	MID	MIV	MRR	MTF
Taft 1	Maximum	0.0586	0.0166	0.0168	**0.0169**	0.017
	Mean	0.0468	0.0152	0.015	0.0152	0.0153
	Std. Deviation	0.007	0.0025	0.0026	0.0024	0.0024
Taft 2	Maximum	0.0636	0.0141	0.0137	**0.0145**	0.0158
	Mean	0.0411	0.0123	0.0119	0.0123	0.0128
	Std. Deviation	0.0113	0.0019	0.0019	0.0019	0.0021
El-centro 1	Maximum	0.0716	0.0198	0.0198	**0.0199**	0.0204
	Mean	0.0556	0.0168	0.0165	0.017	0.0169
	Std. Deviation	0.0083	0.0027	0.0028	0.0028	0.0028
El-centro 2	Maximum	0.0685	0.0184	0.0182	**0.0187**	0.0195
	Mean	0.0495	0.0152	0.0147	0.0154	0.0163
	Std. Deviation	0.0085	0.003	0.0033	0.003	0.0029
Damping ratio %	1st mode		6.08	6.09	5.85	5.97
	2nd mode		11.31	16.08	10.27	6.75
Total dampers installed			80	84	**78**	78

Table 4.2: Simulation Design: Structure 1

	1	2	3	4	5	6	7	8	9	10
MID	20	-	12	20	-	20	-	5	3	-
MIV	12	-	12	20	-	20	5	7	8	-
MRR	20	8	11	12	-	20	4	1	2	-
MTF	16	11	16	17	3	15	-	-	-	-

Table 4.3: Strategic Damper Distribution: Structure 1

Table. (4.3) shows each design's distribution of the damping coefficients.

4.1.2 Case 2

For structure's that have uniformly distributed stiffness, numerous studies have shown that, it is effective when passive energy dissipation device's are distributed in the lower half of the structure. The model in case 2 is a representative model of such case. It is found that all the proposed methods converge to the similar design: distributing devices to the lower half of the structure. Thus, the emphasis here is to check that the designs match with previous studies. Here, we did not evaluate the designs due to the loss of diversity between the designs.

The constraints imposed are:

- Target inter-story strain: $0.02(m)$
- Available Damper per floor (A/F): 30
- Total number of dampers (Tot): 70

Case 2: 70 Tot, 30 A/F

		Init. Values	MID	MIV	MRR	MTF
Taft 1	Maximum	0.0598	0.017	0.017	0.017	0.017
	Mean	0.0424	0.0136	0.0136	0.0136	0.0136
	Std. Deviation	0.0124	0.0043	0.0043	0.0043	0.0043
Taft 2	Maximum	0.0277	0.0138	0.0138	0.0137	0.0138
	Mean	0.0204	0.0115	0.0115	0.0115	0.0115
	Std. Deviation	0.0055	0.0033	0.0033	0.0033	0.0033
El-centro 1	Maximum	0.0543	0.0172	0.0172	0.0171	0.0172
	Mean	0.0397	0.0124	0.0124	0.0124	0.0124
	Std. Deviation	0.0117	0.048	0.0048	0.0048	0.0048
El-centro 2	Maximum	0.0726	**0.0263**	**0.0263**	**0.0263**	**0.0263**
	Mean	0.0478	0.0197	0.0197	0.0197	0.0197
	Std. Deviation	0.0156	0.0078	0.0078	0.0078	0.0078
Damping ratio %	1st mode		6.58	6.58	6.55	6.58
	2nd mode		13.29	13.29	13.81	13.29
Total dampers installed			70	70	70	70

Table 4.4: Simulation Design: Structure 2

However, as illustrated in Table. (4.4), the design criteria is not satisfied. For El-centro 2, the inter-story strains are 0.0263, which indicates that the design needs to be redesigned from the initial stage. Changes in the stiffness or the increase of damping may be an issue. It would be interesting to evaluate cost effects in this sort of problem, where the design process could propose in which direction the redesigning should progress: variation of stiffness or damping?

This case study also indicates that to protect low-rise buildings, which generally may lie in this sort of category of structure's, filling devices from the lower floors may be an accurate *rule by the thumb.*

	1	2	3	4	5	6	7	8	9	10
MID	30	27	13	-	-	-	-	-	-	-
MIV	30	27	13	-	-	-	-	-	-	-
MRR	30	24	15	1	-	-	-	-	-	-
MTF	30	27	13	-	-	-	-	-	-	-

Table 4.5: Strategic Damper Distribution: Structure 2

4.1.3 Case 3

Case 3 is a variation of the stiffness of the previous case. The stiffness is divided into 2 segments. Though, the model seems unrealistic, it does show that efficient design is a function of stiffness as well.

The constraints imposed are:

- Target inter-story strain: $0.02(m)$
- Available Damper per floor (A/F): 30
- Total number of dampers (Tot): 110

Case 3: 110 Tot, 30 A/F

		Init. Values	MID	MIV	MRR	MTF
Taft 1	Maximum	0.0859	0.0156	0.0158	0.0156	0.0155
	Mean	0.0545	0.0126	0.0124	0.0124	0.0125
	Std. Deviation	0.0159	0.0028	0.003	0.003	0.0028
Taft 2	Maximum	0.057	0.0144	0.0134	0.0146	0.0143
	Mean	0.038	0.0112	0.011	0.0109	0.0111
	Std. Deviation	0.0123	0.0023	0.0022	0.0026	0.0024
El-centro 1	Maximum	0.0798	0.0156	0.0159	0.0153	0.0155
	Mean	0.0529	0.0131	0.0129	0.013	0.013
	Std. Deviation	0.0133	0.003	0.0032	0.003	0.0029
El-centro 2	Maximum	0.0357	0.02	0.0201	0.0198	0.0198
	Mean	0.0255	0.015	0.0151	0.0149	0.015
	Std. Deviation	0.0063	0.0045	0.0045	0.0045	0.0045
Damping ratio %	1st mode		10.75	10.36	10.39	10.65
	2nd mode		78.56	79.41	84.86	81.8
Total dampers installed			110	110	110	110

Table 4.6: Simulation Design: Structure 3

	1	2	3	4	5	6	7	8	9	10
MID	30	25	-	-	-	30	24	1	-	-
MIV	23	15	6	1	-	30	23	12	-	-
MRR	27	22	15	-	-	30	14	2	-	-
MTF	30	23	7	-	-	30	20	-	-	-

Table 4.7: Strategic Damper Distribution: Structure 3

4.1.4 Case 4

As shown in Table. (4.1), this case is just another stiffness variation from the previous cases: the sum of stiffness and mass are the same. This model distributes the stiffness, in order to obtain a uniform 1^{st} mode-shape.

The constraints imposed are:

- Target inter-story strain: $0.02(m)$
- Available Damper per floor (A/F): 15
- Total number of dampers (Tot): 75

With these constraints specified in the design, the strategic indices are evaluated. Fig. (4-2)

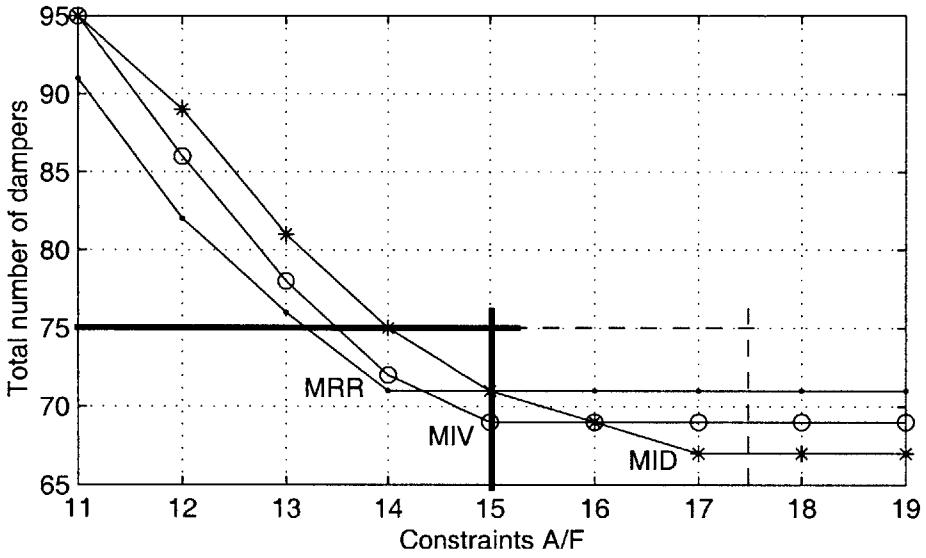

Figure 4-2: Design evaluation: Case 4

illustrates the comparison of the proposed methods for case 4. The MRR index shows to be the better design till 14 A/F, where it falls into the limit. For 15 A/F, MIV becomes the better design, but there after MID becomes the most preferable without any Tot and A/F constraints. The limitation for MID is 17 A/F with 67 total dampers installed.

If the A/F and Tot constraints are imposed the optimal design is given inside the squared area. In this case, several designs are available. However, MIV (15) becomes the overall optimal design with 69 total dampers installed.

Case 4: 75 Tot, 15 A/F

		Init. Values	MID	MIV	MRR	MTF
Taft 1	Maximum	0.2061	0.0195	**0.019**	0.0192	0.0191
	Mean	0.074	0.0161	0.0162	0.016	0.0162
	Std. Deviation	0.0565	0.0031	0.0032	0.0031	0.0032
Taft 2	Maximum	0.1344	0.016	**0.0159**	0.0159	0.0159
	Mean	0.0455	0.0136	0.0137	0.0136	0.0137
	Std. Deviation	0.0369	0.0025	0.0026	0.0025	0.0026
El-centro 1	Maximum	0.1583	0.0198	**0.0198**	0.0199	0.0197
	Mean	0.0621	0.0163	0.0166	0.0164	0.0165
	Std. Deviation	0.0411	0.0034	0.0036	0.0036	0.0036
El-centro 2	Maximum	0.149	0.0188	**0.0187**	0.0187	0.0187
	Mean	0.0675	0.0162	0.0162	0.016	0.0162
	Std. Deviation	0.036	0.0024	0.0025	0.0025	0.0026
Damping ratio %	1st mode		8.61	8.54	8.73	8.57
	2nd mode		72.07	87.05	87.27	87.05
Tota dampers installed			71	**69**	71	69

Table 4.8: Simulation Design: Structure 4

	1	2	3	4	5	6	7	8	9	10
MID	-	-	-	-	6	15	15	15	13	7
MIV	-	-	-	-	9	13	15	15	11	6
MRR	-	-	-	-	12	14	14	14	11	6
MTF	-	-	-	-	7	15	15	15	11	6

Table 4.9: Strategic Damper Distribution: Structure 4

4.1.5 Case 5

The constraints imposed are:

- Target inter-story strain: $0.02(m)$
- Available Damper per floor (A/F): 15
- Total number of dampers (Tot): 75

With these constraints specified in the design, the strategic indices are evaluated. Fig. (4-3)

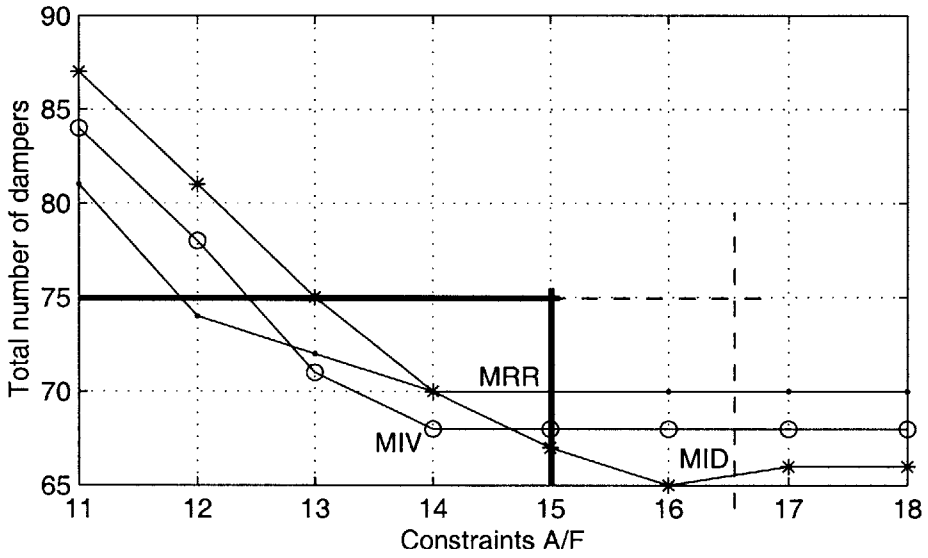

Figure 4-3: Design evaluation: Case 5

illustrates the comparison of the proposed methods for case 5. The MRR index shows to be the better design till 12 A/F, where it falls into the limit. For $13 \sim 14$ A/F, MIV becomes the better design, but there after MID becomes the most preferable without any Tot and A/F constraints. Without any constraints imposed the MID's best design is at 16 A/F, with only 65 total dampers installed.

If the A/F and Tot constraint are imposed the optimal design is given inside the squared area. In this case, the MID (15) becomes the overall optimal design with 69 total dampers installed.

Case 5: 75 Tot,15 A/F

		Init. Values	MID	MIV	MRR	MTF
Taft 1	Maximum	0.1395	**0.0187**	0.0183	0.0185	0.0186
	Mean	0.0554	0.0161	0.0159	0.0158	0.016
	Std. Deviation	0.0388	0.003	0.003	0.0029	0.003
Taft 2	Maximum	0.1692	**0.017**	0.0165	0.0168	0.0168
	Mean	0.0656	0.0143	0.0143	0.0142	0.0143
	Std. Deviation	0.044	0.0028	0.0028	0.0027	0.0028
El-centro 1	Maximum	0.0986	**0.0196**	0.0198	0.0195	0.0194
	Mean	0.0447	0.0168	0.0165	0.0163	0.0167
	Std. Deviation	0.0256	0.0027	0.0028	0.0028	0.0027
El-centro 2	Maximum	0.1119	**0.0199**	0.0199	0.0197	0.0199
	Mean	0.0424	0.0173	0.0171	0.0169	0.0173
	Std. Deviation	0.03	0.0026	0.0026	0.0025	0.0026
Damping ratio %	1st mode		8.67	8.84	9.02	8.73
	2nd mode		76.34	86.81	86.81	81.69
Total dampers installed			**67**	68	70	67

Table 4.10: Simulation Design: Structure 5

	1	2	3	4	5	6	7	8	9	10
MID	-	-	-	-	4	15	15	15	12	6
MIV	-	-	-	-	10	13	15	14	10	6
MRR	-	-	-	-	13	14	13	14	10	6
MTF	-	-	-	-	5	15	15	15	11	6

Table 4.11: Strategic Damper Distribution: Structure 5

Damping Ratio

Obtaining the target damping ratio in structural dynamics is the first step in design. However, to obtain a target damping ratio for a MDOF system is not a simple task. In addition, to find the proper damping for both the 1^{st} and 2^{nd} mode, would make the problem unsolvable via a analytic method. As illustrated in Table. (4.2) $\sim$ Table. (4.10), even when damping ratios are within a target, the efficiency or effect of the dampers on the response differ. Eventually, higher damping ratio does not directly indicate a better design, as shown in Table. (4.10).

4.1.6 Strategic Distribution

The objective of this study was to distribute the damping coefficients in a strategic manner. Table. (4.3) $\sim$ Table. (4.11) show the obtained distribution of the coefficients. We may observe that while the designs differ from each other, they do match a trend that fits each structure. For example, all the methods prefer to place devices in the lower half of the structure for the uniformly distributed case 2. While, in case 4 and 5, the designs show that placing devices on the upper half is desirable.

Fig. (4-4) to Fig. (4-6) show the effectiveness of the reduction induced by the strategic placements of energy dissipation devices. The floors where the maximum inter-story drifts occurred were taken.

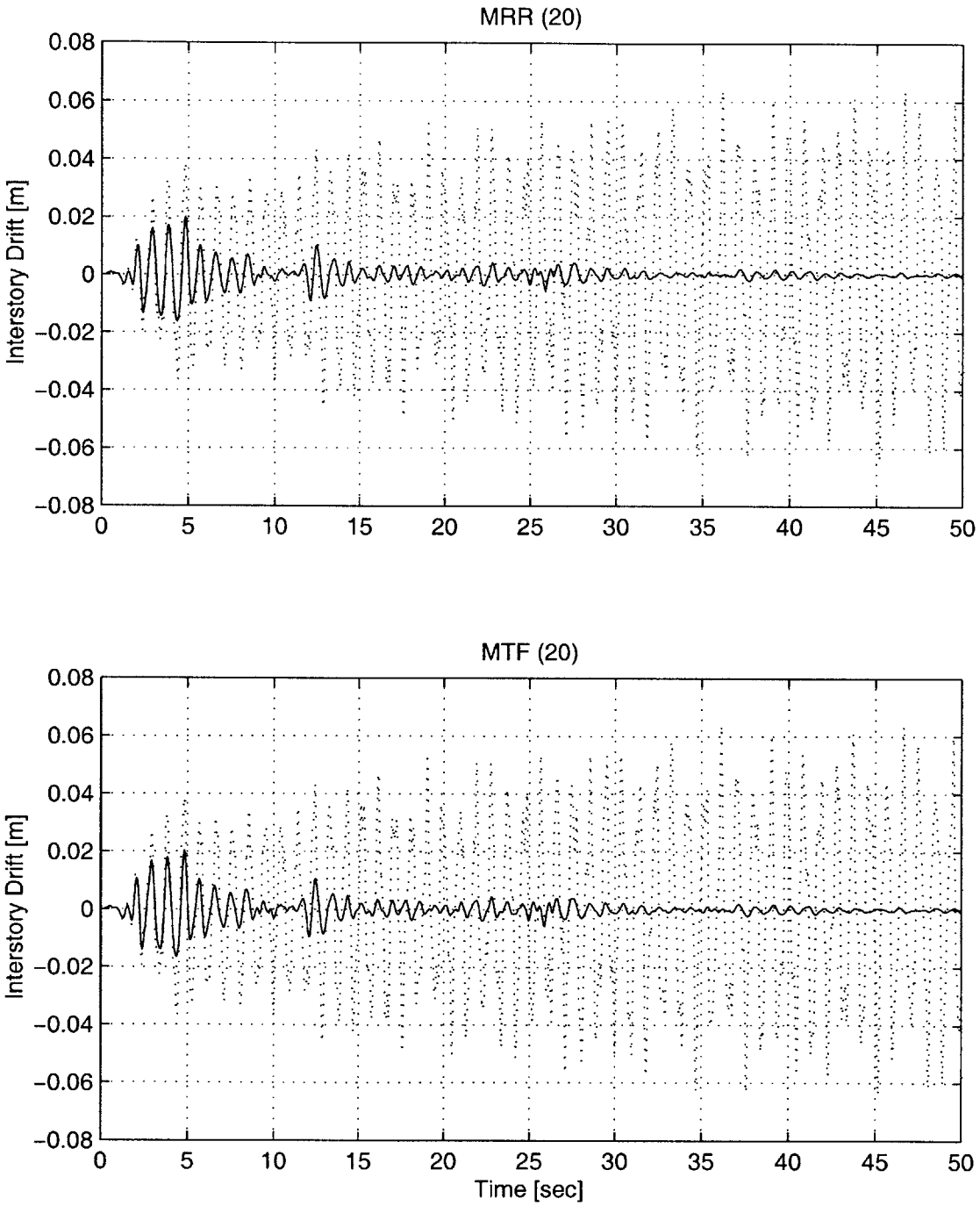

Figure 4-4: Case 1: Time history of Floor 6 (El-centro S90W)

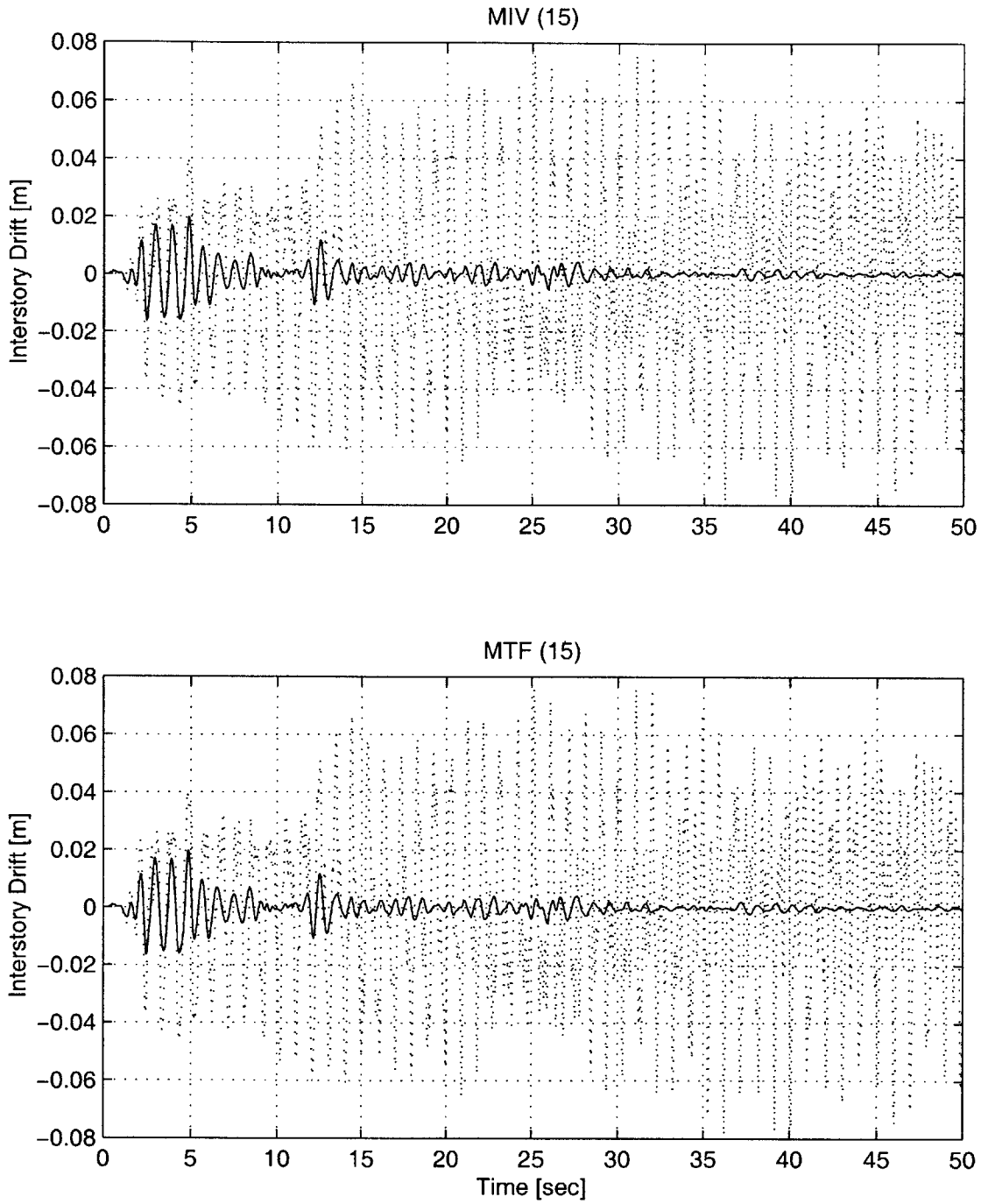

Figure 4-5: Case 4: Time history of Floor 8 (El-centro S90W)

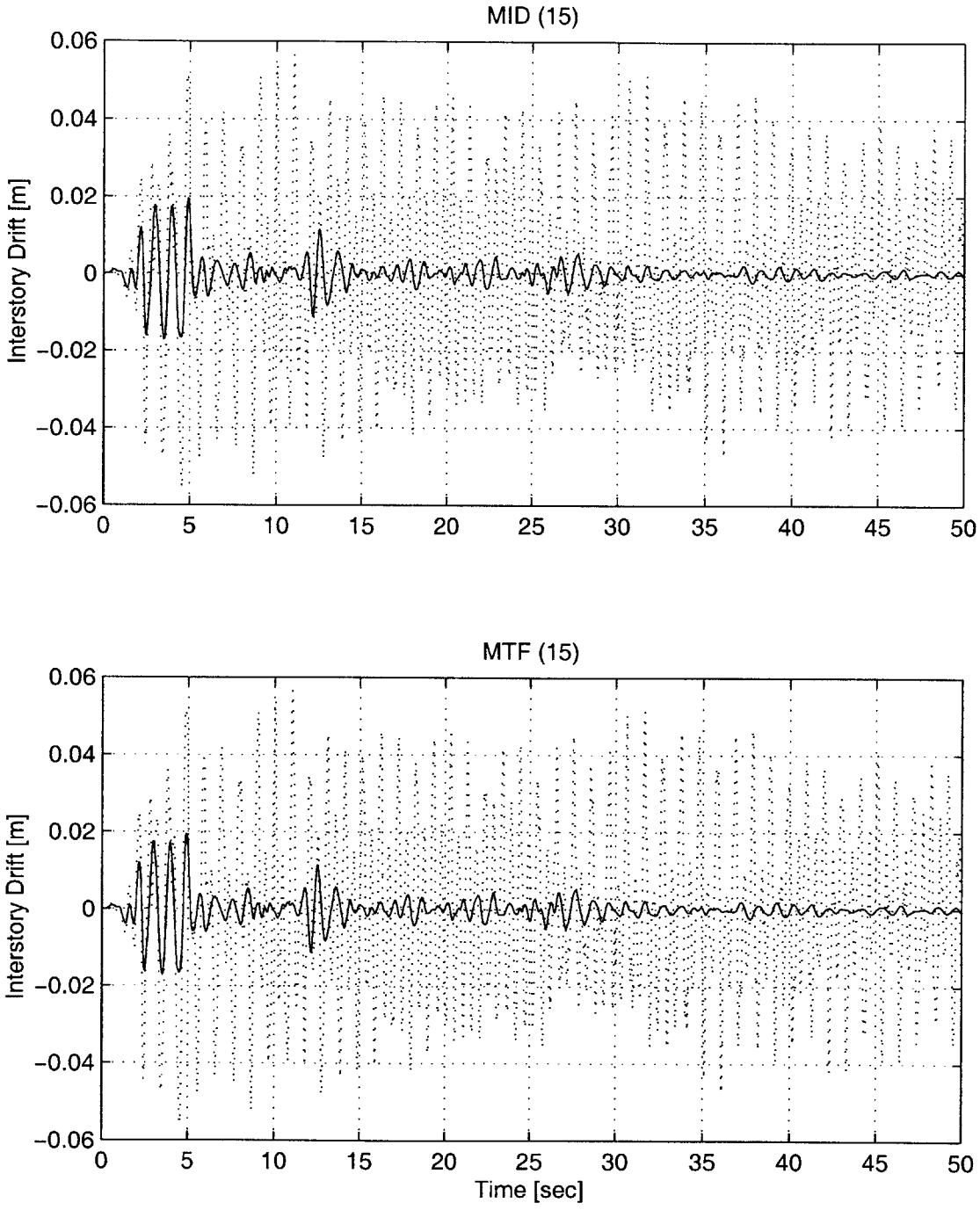

Figure 4-6: Case 5: Time history of Floor 8 (El-centro S90W)

4.2 Search Technique: Minimization of Transfer Functions (MTF)

4.2.1 Application: case 6 and 7

Here, we compare a general approach, which minimizes the transfer function. We take the model and results used in [13] to compare with the MTF.

The responses are given in Table. (4.12) and Table. (4.13). We may observe that the proposed method has obtained a similar design suggested by Takewaki [13]. The maximum interstory drifts were actually less than the compared design.

Taking case 6 we may observe that the structure has a uniformly distributed stiffness in Table. (4.1). It has been suggested that in such cases, placing energy dissipation devices at the lower half is efficient. As illustrated in Table. (4.12), both designs coincide with the trend, placing devices in the lower floors. The only difference is that the MTF distributes a small amount of damping in floor 3. Hence, it obtains a slightly better response then the other method. In both of the designs the damping ratio are similar. However, a difference can be observed in the second mode.

Takewaki							MTF						
1	2	3	4	5	6	Floors	1	2	3	4	5	6	
4.8	4.2	-	-	-	-	Distribution	4.8	3.6	0.6	-	-	-	
Taft 1	Taft 2	El-cen 1	El-cen 2			-	Taft 1	Taft 2	El-cen 1	El-cen 2			
0.0199	0.0167	0.0202	0.0278			Maximum	0.0197	0.0165	0.0188	0.0272			
0.0166	0.0144	0.016	0.0221			Mean	0.0162	0.0141	0.0152	0.0217			
0.0044	0.0028	0.0045	0.0071			Std. dev	0.0045	0.003	0.0045	0.0074			
1^{st}mode	17.74	2^{nd}mode	61.33			Damp. ratio	1^{st}mode	17.3	2^{nd}mode	66.65			

Table 4.12: MTF: Structure 6

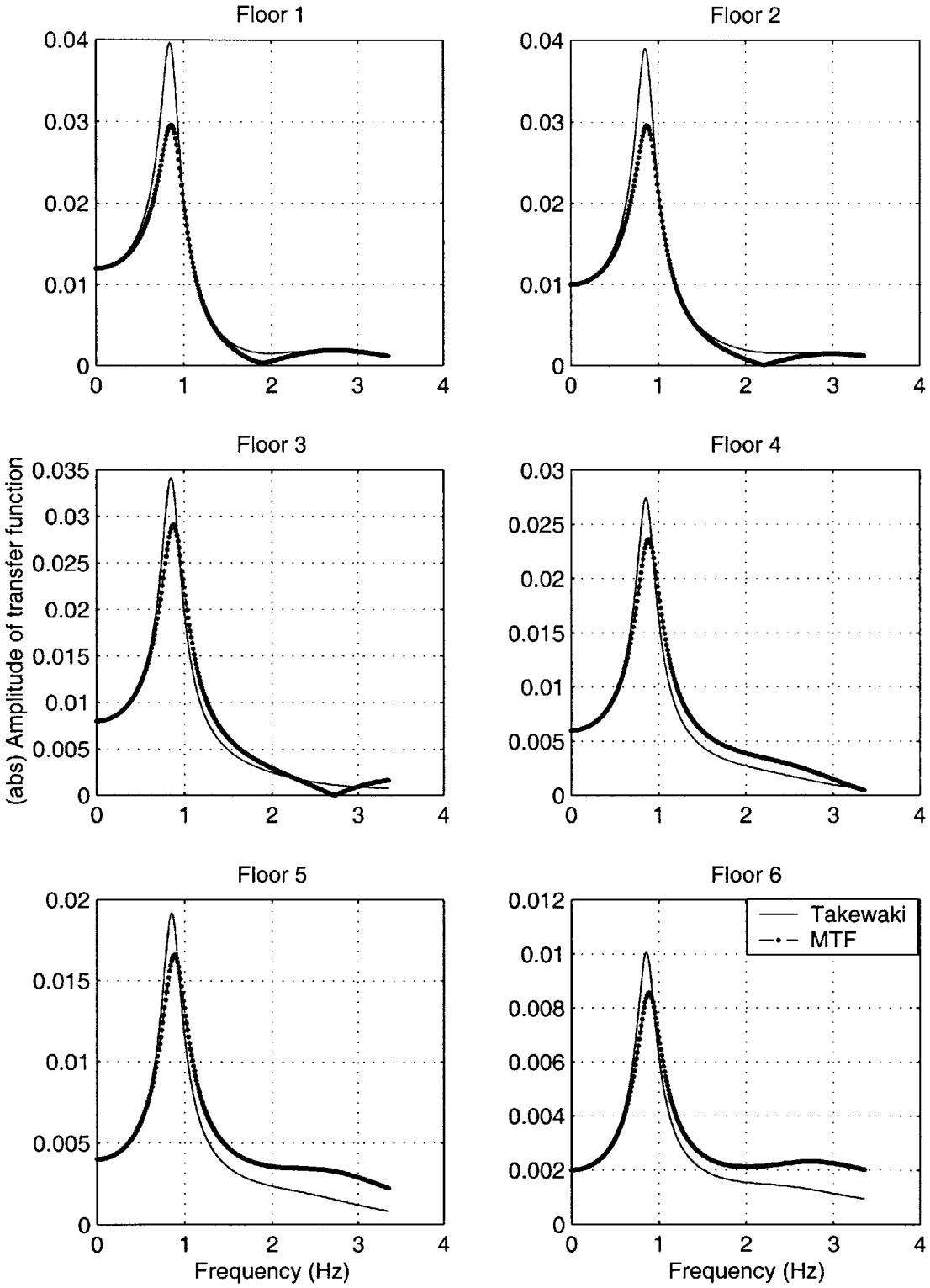

Figure 4-7: Comparison of (abs) Transfer functions: Case 6 (Floor 1,2,3,4,5,6)

Fig. (4-7) compares the obtained transfer functions. It is clear that the maximum amplitude of the transfer function has been reduced. This gave rise to a better performance against the excitations. Especially, against El-centro 2, where the maximum inter-story drift reduced 9.3%. Although, we may observe that in the higher frequencies, the amplitude of the transfer functions have increased. However, the objective to minimize the maximum amplitudes of the transfer functions have been achieved.

In case 7 the stiffness was redistributed in order to have a uniform distribution of the amplitudes of transfer functions of inter-story drifts. The design in this example differs more than the previous example. As illustrated in Fig. (4-8), the maximum amplitudes of the transfer functions have been reduced. However, we may notice that the amplitude of the transfer function has been increased for the 6^{th} floor.

Takewaki							MTF						
1	2	3	4	5	6	Floors	1	2	3	4	5	6	
13	9	19	18	17	14	Distribution	15	15	13.5	15	15	16.5	
Taft 1	Taft 2		El-cen 1		El-cen 2	-	Taft 1	Taft 2		El-cen 1		El-cen 2	
0.0196	0.0168		0.0176		0.0274	Maximum	0.0196	0.0173		0.0172		0.0271	
0.0192	0.0164		0.0169		0.0267	Mean	0.019	0.0161		0.0169		0.0266	
0.00029	0.00037		0.00039		0.0006	Std. dev	0.00039	0.00082		0.00025		0.00043	
1^{st}mode	12.27		2^{nd}mode		100.4*	Damp. ratio	1^{st}mode	12.05		2^{nd}mode		76.37	

Table 4.13: MTF: Structure 7

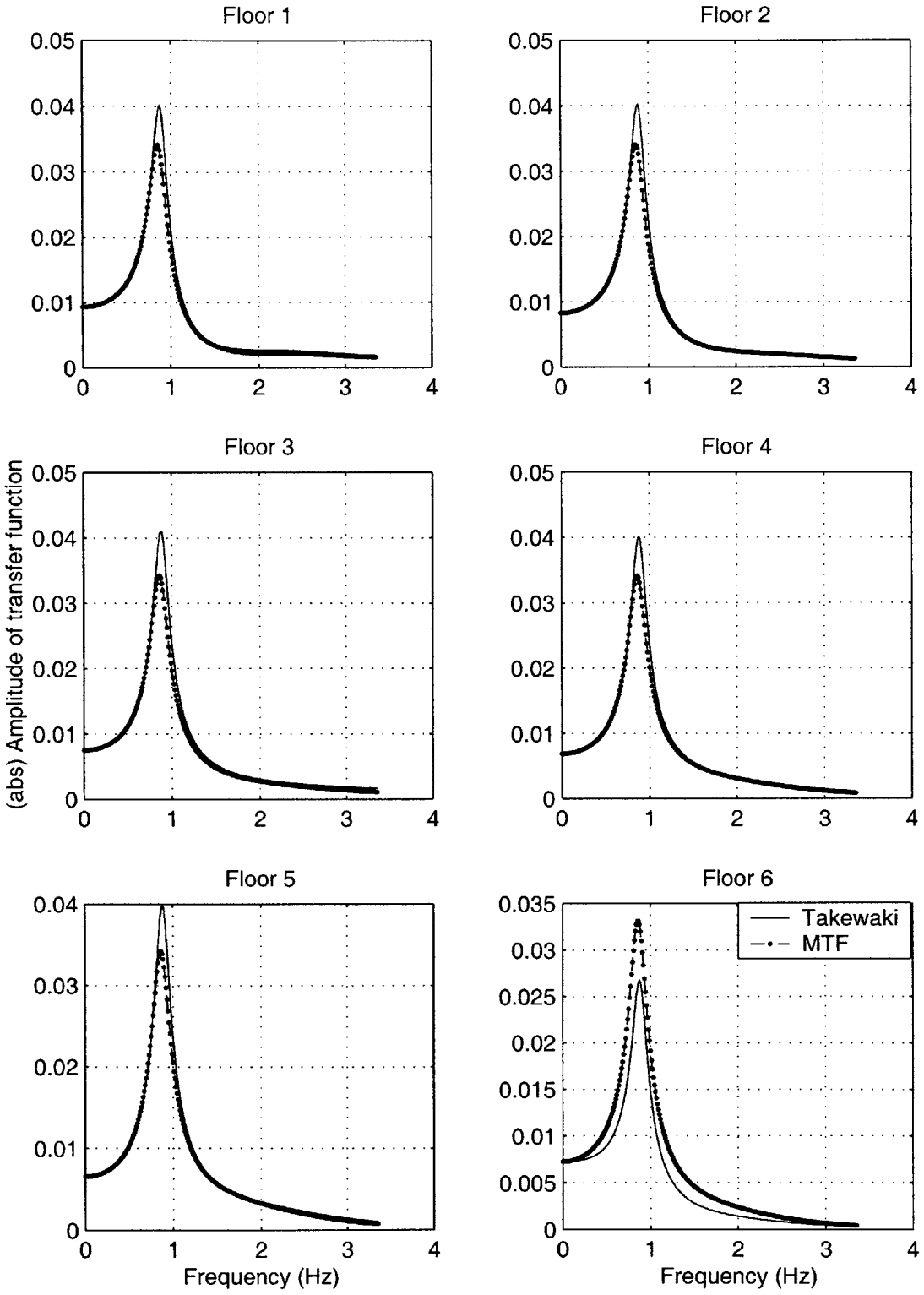

Figure 4-8: Comparison of (abs) Transfer functions: Case 7 (Floor 1,2,3,4,5,6)

4.2.2 Transfer Functions

The MTF method, like most nonlinear solving techniques, is not a robust solution technique, due to the necessity of a good initial guess it requires. The method is effective when used in case 6 and 7. However, when applied to the previous cases with the strict constraints applied, the results are not as satisfactory. This is mostly due to the characteristic of the method, which makes it difficult to impose any strict constraints during the search. However, by modifying the search algorithm, this obstacle can be avoided. In Table. (4.8) and Table. (4.10), the results of the MTF were actually better than the optimal designs, MIV (15) and MID (15), respectively. The MTF method also distinguished itself, when compared with the best designs without any constraints. For example, in case 4, when given 67 total dampers the method converged to the same design as the MID (17). For case 5, it again converged to the exact design provided by MID (16). It should be noted that the MID (16) design was only obtained due to the imposed 16 A/F constraint. This is proved by the fact that it did not provide the same design in MID (17), which is the actual limit for the MID in case 5.

		1	2	3	4	5	6	7	8	9	10
Case 1	MRR (25)	18	8	6	13	-	25	1	-	2	-
	MTF* (25)	15	11	14	16	3	13	1	-	-	-
Case 4	MID (17)	-	-	-	-	-	15	17	17	12	6
	MTF (17)	-	-	-	-	-	15	17	17	12	6
Case 5	MID (16)	-	-	-	-	2	14	16	16	11	6
	MTF (16)	-	-	-	-	2	14	16	16	11	6

Table 4.14: Best Designs *Vs* MTF

However, in addition to the drawback on strict constraints another phenomena may be observed in case 1, MTF*. After the initial guess, which considers the lower modes, the MTF solution technique scans through the n dimensional space, which is consisted with the maximum amplitudes of the transfer functions.

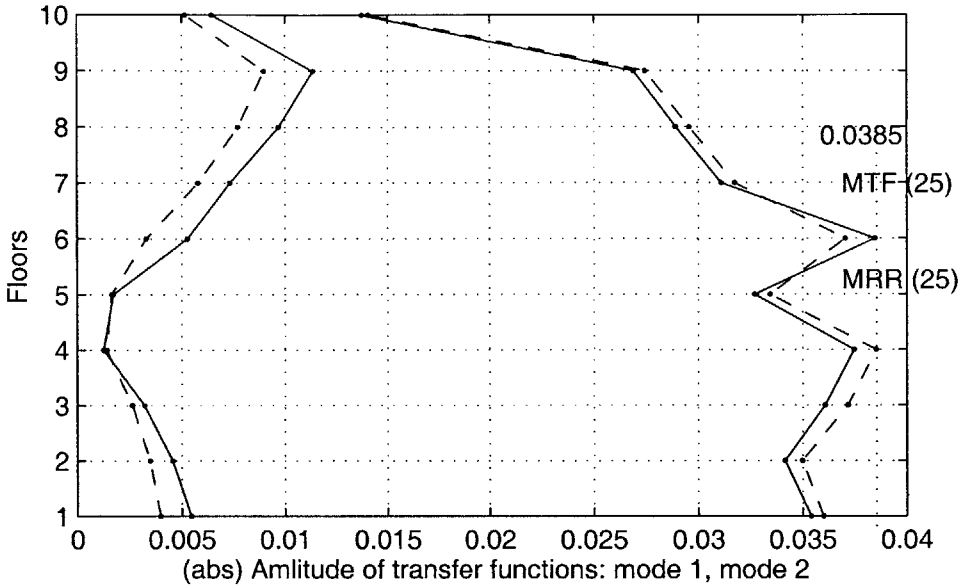

Figure 4-9: Comparison of peak (abs) Transfer functions in Case 1: MTF (25) and MRR (25)

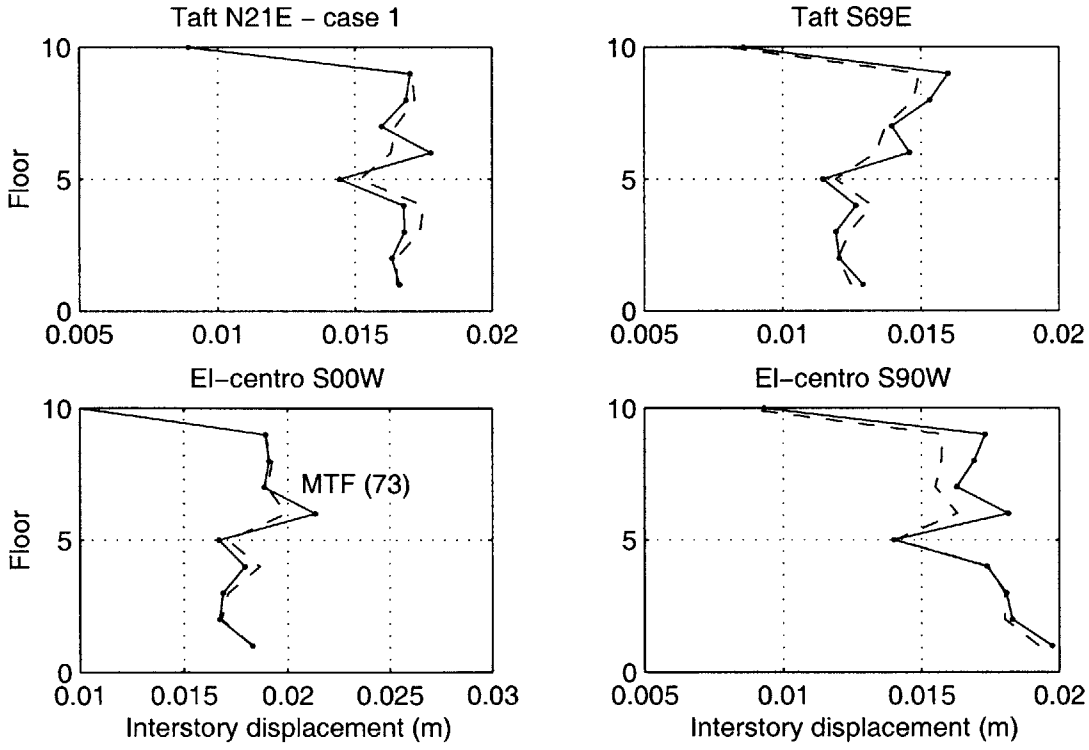

Figure 4-10: Comparison of response in Case 1: MTF (25) and MRR (25)

The MTF solution technique actually finds a distribution which gives a better solution compared with the MRR (20). This is true only when the maximum amplitudes of the transfer functions are compared. The response of the structure is totally a different story as shown in Table. (4.2).

When again compared with the MRR (25), the same occurs. As illustrated in Fig. (4-9), the amplitude of the transfer functions of the 1^{st} mode is reduced, however, in the higher frequencies there has been an amplification. In Fig. (4-10), the inter-story displacements due to the 4 earthquakes are shown. Under El-centro S00W, the MTF (25) does not satisfy the design constraints. And as expected it is the 6^{th} floor that fails.

This problem occurs due to the limitation of the ability to control an MDOF system. It seems that mathematically, obtaining the minimum amplitude of the transfer function is not sufficient, due to the possibilities that higher modes may be excited. There exists no analytical solution to consider those contributions in a MDOF system. This phenomena may give the upper hand to simulation design, due to the ability to consider the characteristic of the external excitations.

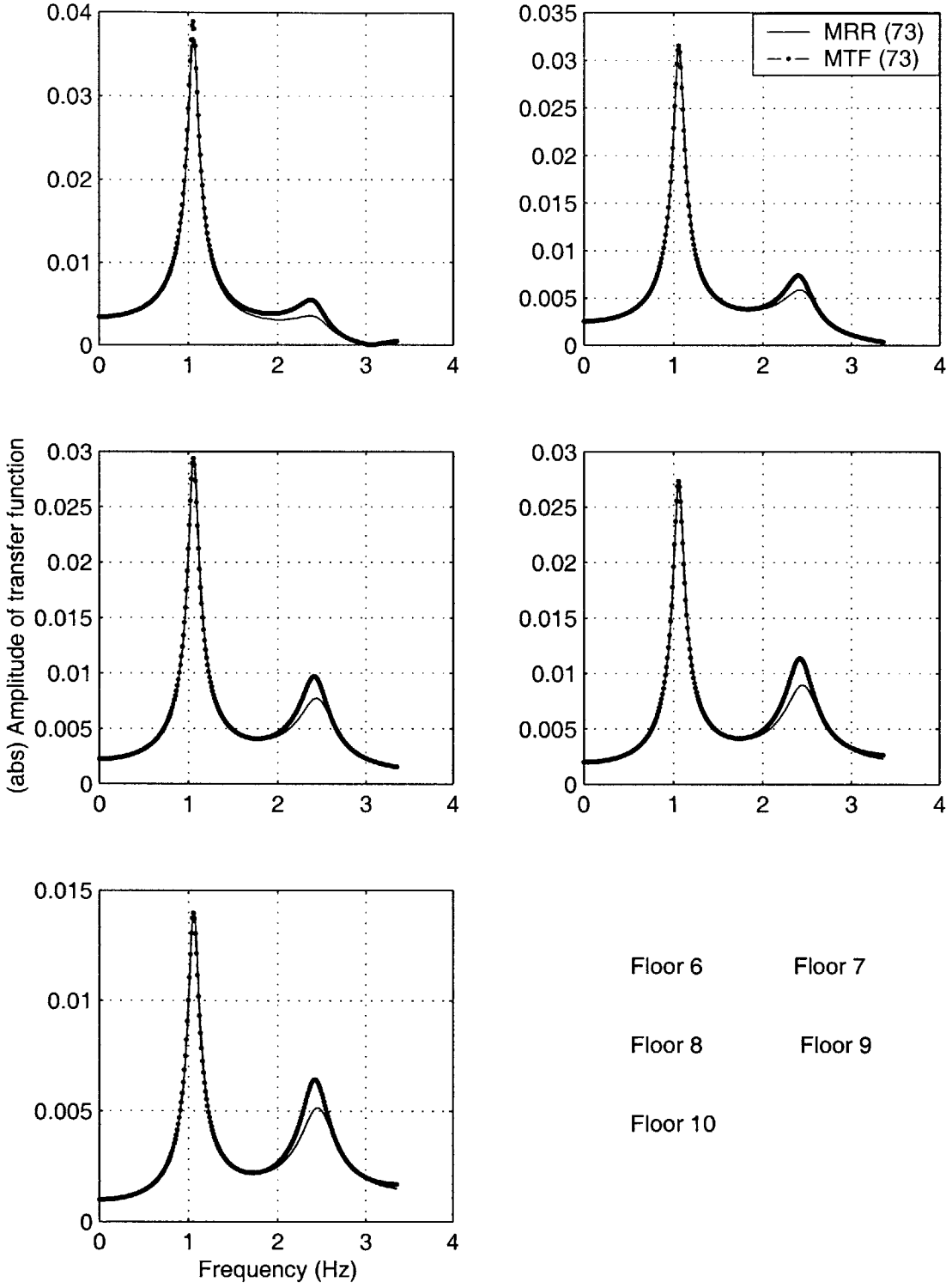

Figure 4-11: Comparison of (abs) Transfer functions: Case 1 (Floor 6,7,8,9,10)

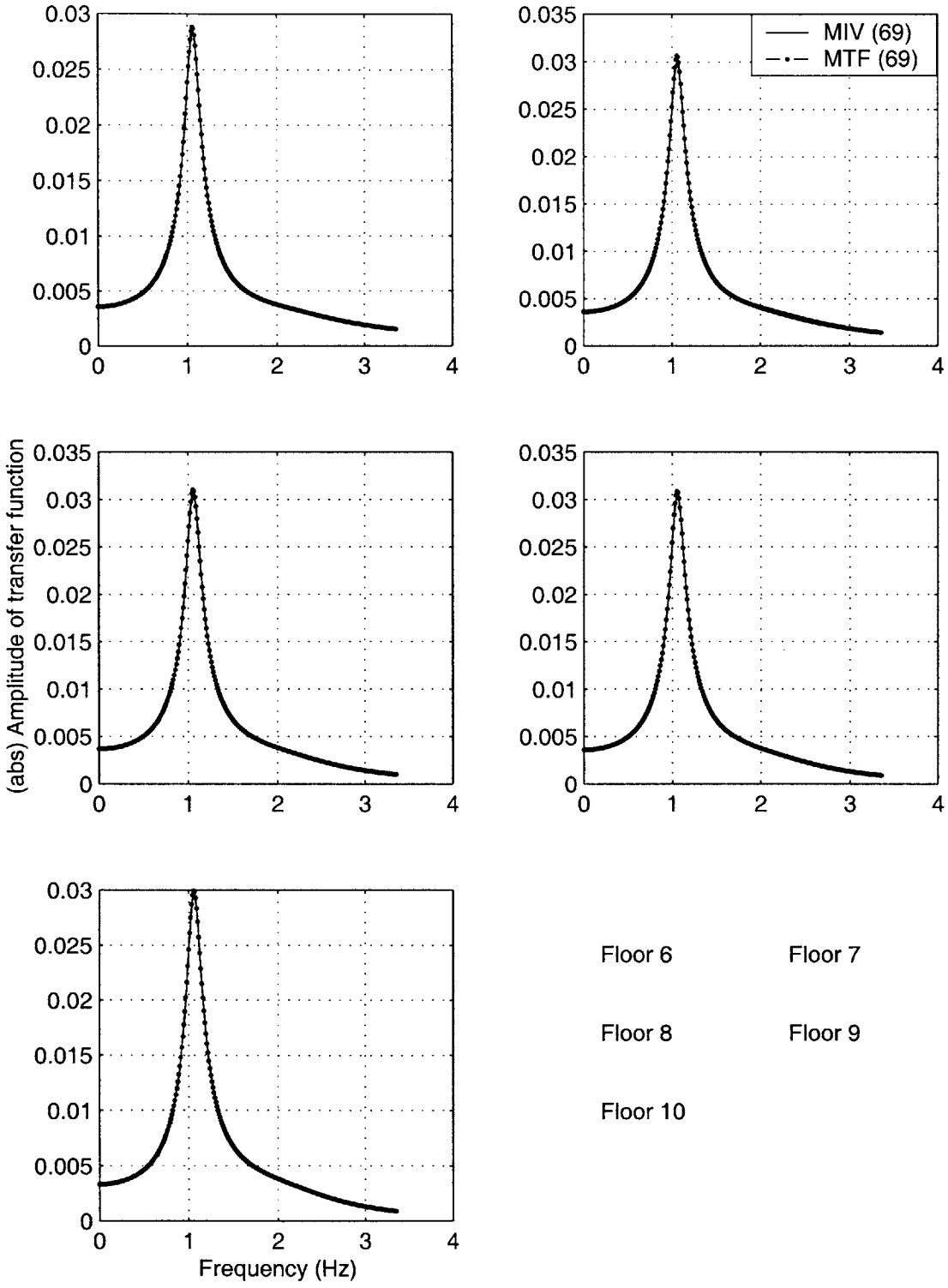

Figure 4-12: Comparison of (abs) Transfer functions: Case 4 (Floor 6,7,8,9,10)

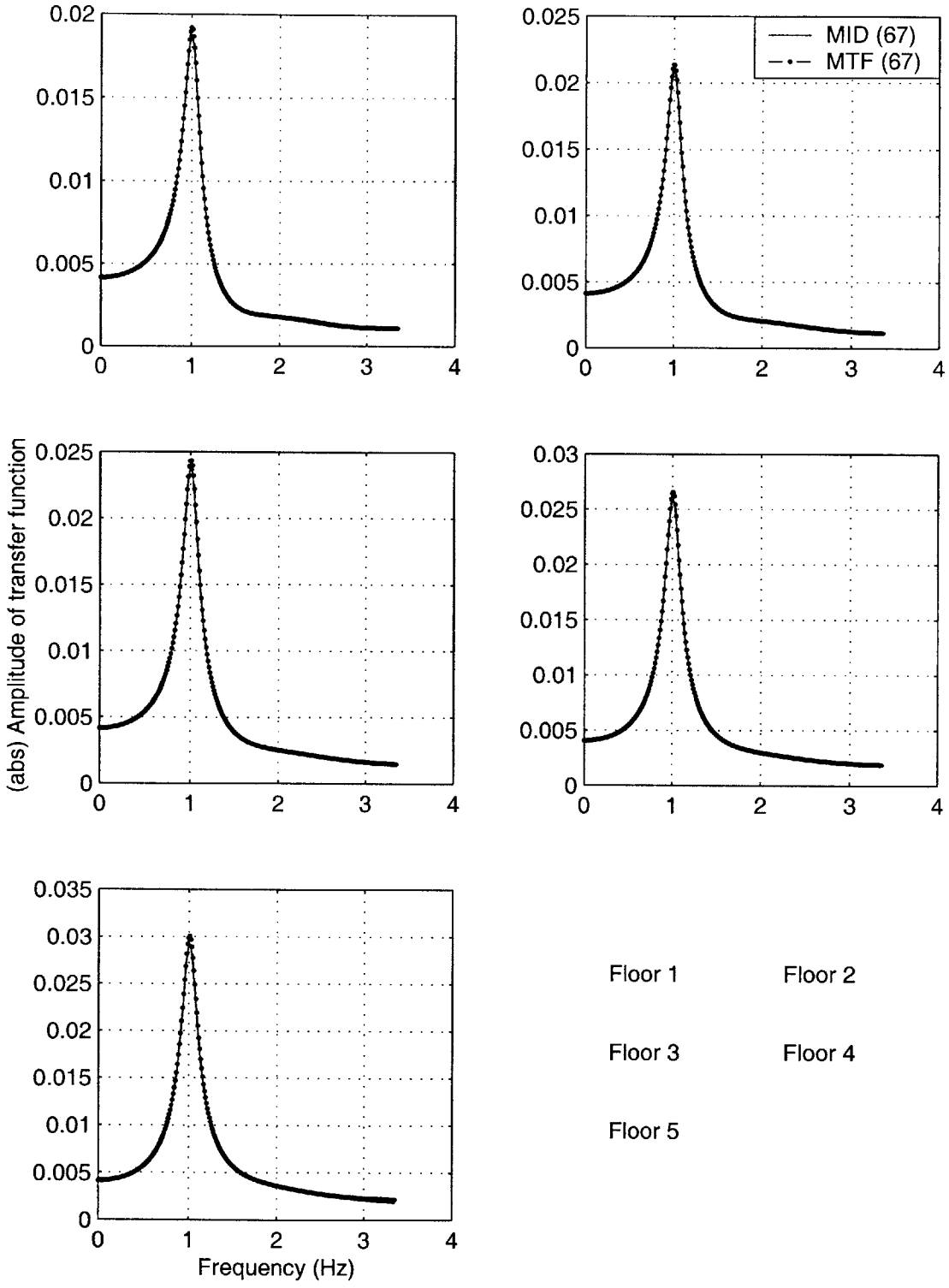

Figure 4-13: Comparison of (abs) Transfer functions: Case 5 (Floor 1,2,3,4,5)

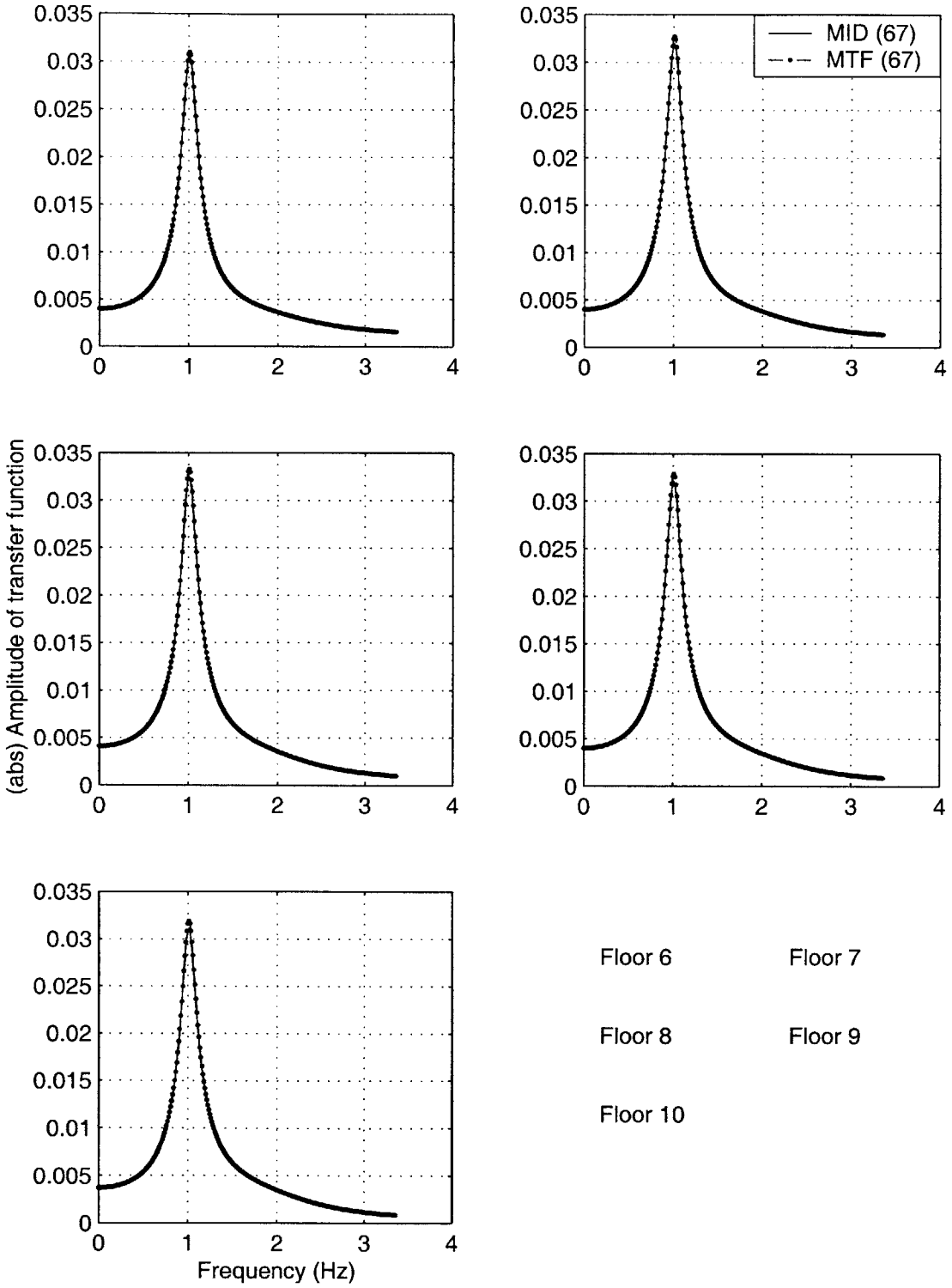

Figure 4-14: Comparison of (abs) Transfer functions: Case 5 (Floor 6,7,8,9,10)

Chapter 5

Conclusion

5.1 Summary

The new concept of structural design, which incorporates structural protection systems, has emerged in the last decade. In addition, the need to implement this approach in a systematic method also has been exploited in numerous studies. Here, a simulation design method and search technique, which utilizes the general dynamic property, was examined.

The definition of *Optimality* was defined by obtaining the better response, with a constraint on the sum of the damping coefficients. The objective of the study was to determine the optimal distribution of the damping coefficients of the system. Cost effects which is another important issue that must be considered in practical usage was inverted into a constraint problem. It showed to blend in well into the simple algorithms of the proposed methods.

5.1.1 Simulation Design

The simulation design method uses strategic indices to help find the optimal positions of the damping coefficients. Various strategic indices were examined and proposed: MID, MIV, MRR.

- MID: This index indicates the floor with the maximum inter-story drifts
- MIV: This index indicates the floor with the maximum inter-story velocity
- MRR: This index indicates the floor which has the maximum effect/reduction on the previous maximum inter-story drift

All of these indices proved to work well, although their designs differ. The MRR seem to have the most impact on strict A/F constraints, while the MID seems to have consistency. Thus, the MID provided the best designs when the A/F constraints were more or less withdrawn.

The simulation design process proved to be effective when various constraints were to be imposed due to its simple algorithm. This is an advantage which the MTF approach has failed.

5.1.2 Search Technique

The search technique (MTF) was used to provide a general solution to the given problem. The objective was to minimize the maximum absolute amplitude of the transfer function. Thus, the obtained solution does not rely on external excitations.

To obtain the transfer function of the structure, the chain structure model was used. This method is only applicable to structures that can be modified as an FEM model. Allowing to determine the response of the structure when the end boundary conditions are imposed. This eventually leads to the transfer function.

Another important aspect to this method is to start with a good initial guess. However, by using basic dynamic characteristics: protecting the fundamental mode, this seems to have been achieved. The MTF method has provided more desirable designs compared to the simulation design method in all but case 1. This was due to the lack of controllability over the higher modes. This evidently could become an important issue, due to the characteristics of the external excitations.

The most significant draw back on this method is the heavy computational intensity compared to the simulation design approach. Another demerit for this approach would be the lack of control on the higher modes.

5.2 Further Comments

Cost, as well as performance, is an essential element and constraint in design. While evaluating the distribution of the damping coefficients, the cost factors have been transformed into a constraint problem which was then applied to the the problem. However, to apply the examined methods in practical design schemes, costs factors must be considered in a more

sophisticated matter. What should the capacity devices be? Which dissipation devices should be used? are some initial decisions to start with in the design process. While cost of damping devices accelerates as the required capacity increases, introducing penalty factors where large damping concentrates, could also improve the design. In addition, installing costs may also be considered, as well as, repair/maintenance costs to improve the design.

Finally, to achieve the ultimate goal for efficient design, the design should also consider the stiffness distribution. Thus, to consider stiffness as well in the overall design process would be a requirement.

Bibliography

[1] Seshasayee Ankireddi and Henry T.Y. Yang. Multiple objective lqg control of wind-excited buildings. *Journal of Structural Engineering*, 1997.

[2] Ray W. Clough and Joseph Penzien. *Dynamics of Structures.* McGraw-Hill, Inc., 2^{nd} edition, 1993.

[3] J.J. Connor and B.S. Klink. *Introduction to Motion Based Design.* Computational Mechanics Publications, 1996.

[4] Paul M. DeRusso, Rob J. Roy, Charles M. Close, and Alan A. Desrochers. *State Variables for Engineers.* John Wiley & Sons, INC., 2^{nd} edition, 1998.

[5] N. Gluck, A.M. Reinhorn, J. Gluck, and R. Levy. Design of supplemental dameprs for control of structures. *Journal of Structural Engineering*, 1996.

[6] Raymond G. Jacquot. *Modern Digital Control Systems.* Marcel Dekker, INC., 2^{nd} edition, 1995.

[7] Eduardo Kausel and Jose Roësset. Frequency domain analysis of undamped systems. *Journal of Engineering Mechanics*, 1992.

[8] Jose Luis Mendoze Zabala. State-space formulation for structural dynamics. Master's thesis, Massachusetts Institute of Technology, May 1996.

[9] William H Press, Saul A Teukolsky, William T Vetterling, and Brian P Flannery. *Numerical Recipes in FORTRAN: The Art of Scientific Conputing.* Cambridge University Press, 2^{nd} edition, 1994.

[10] A.K. Shukla and T.K. Datta. Optimal use of viscoelastic dampers in building frames for seismic force. *Journal of Structural Engineering*, 1999.

[11] T.T. Soong and G.F. Dargush. *Passive Energy Dissipation Systems in Structural Engineering.* John Wiley & Sons Ltd, 1997.

[12] Gilbert Strang. *Introduction to Applied Mathematics.* Wellesly-Cambridge Press, 1986.

[13] Izuru Takewaki. Opitmal damper placement for minimum transfer functions. *Earthquake Engineering and Structural Dynamics*, 1997.

[14] Senol Utku. *Theory of Adaptive Structures: Incorporating Intelligence into Engineered Products.* New Directions in Civil Engineering. CRC Press, 1998.

[15] Chun-Yi Wang. Dynamic simulation tool for seismic analysis. Master's thesis, Massachusetts Institute of Technology, may 1998.

[16] Ri-Hui Zhang and T.T. Soong. Seismic design of viscoelastic dampers for structural applications. *Journal of Structural Engineering*, 1992.